Magnetic Films: Studies of the FePt and FeRh systems

Cheikh Birahim Ndao

Supervisors :
Nora Dempsey and Dominique Givord
Nanosciences Department,
Institut Néel CNRS-UJF

Graduation committee :
Véronique Pierron-Bohnes, IPCMS (Strasbourg)
Massimo Ghidini, DMSM (Cambridge)
Aboubaker-Chedikh Beye, GPSSM (Dakar)
Alain Schuhl, Institut Néel (Grenoble)

MEMS (micro-electro-mechanical-systems)

- Collective fabrication with µelectronics technologies (<1mm)
- Several applications : µ-switches, µ-motors, accelerometers…

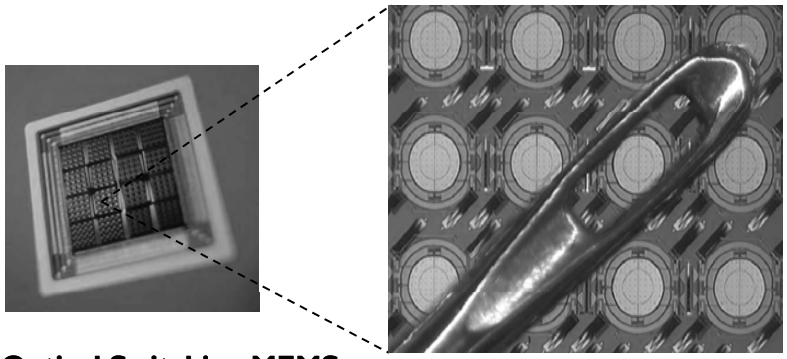

Optical Switching MEMS
Alcatel-Lucent Technologies

Activation in MEMS

- Physical principles used in MEMS
  - Electrostatic
  - Thermal
  - Piezoelectric
  - Magnetostrictive
  - Magnetic

Electrostatic actuation

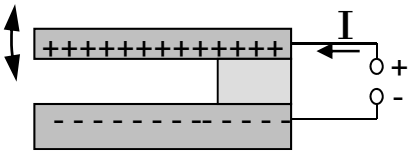

Advantage

Known materials
Easy integration

Disadvantage

short distance+ low force
= **low power**

Magnetic actuation

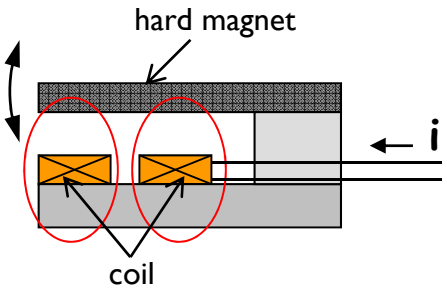

Advantage

long distance+ strong force
= **high power**

Force ~ field gradient
⇒ favours small size

Disadvantage

Difficulty of integration
Complex design

MEMS (micro-electro-mechanical-systems)

- Collective fabrication with µelectronics technologies (<1mm)
- Several applications : µ-switches, µ-motors, accelerometers…

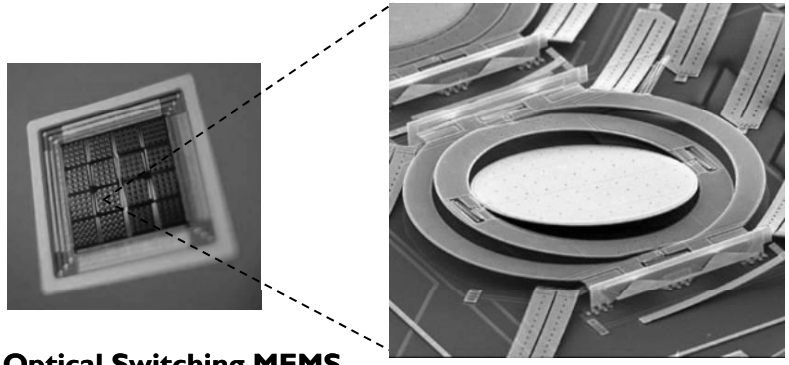

Optical Switching MEMS
Alcatel-Lucent Technologies

Activation in MEMS

- Physical principles used in MEMS
  - Electrostatic
  - Thermal
  - Piezoelectric
  - Magnetostrictive
  - Magnetic

Electrostatic actuation

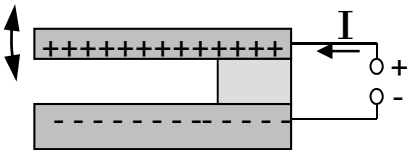

Advantage

Known materials
Easy integration

Disadvantage

short distance+ low force
= **low power**

Magnetic actuation

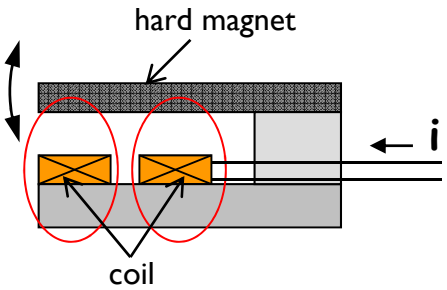

Advantage

long distance+ strong force
= **high power**

Force ~ field gradient
⇒ favours small size

Disadvantage

Difficulty of integration
Complex design

High performance permanent magnet materials

Material	$\mu_0 M_S$ (T)	$\mu_0 H_A$ (T)	$(BH)_{max,th}$ (kJ/m^3)	T_C (K)
RE-TM				
$Nd_2Fe_{14}B$	1.61	7.6	514	585
Sm_2Co_{17}	1.30	6.4	333	1173
$SmCo_5$	1.05	40	220	1000
$L1_0$				
FePt	1.43	11.6	407	750
FePd	1.38	3.3	379	760
CoPt	1.00	4.6	200	840

Thesis
A. Walther
(Néel / LETI / G2Elab)

$L1_0$ vs RE-TM

- Comparable intrinsic magnetic properties
- $L1_0$ alloys much less susceptible to oxidation

Presentation outline

- Sample preparation
- The FePt System
  - Experimental results
  - Analysis
- The FeRh System
  - Experimental results
  - Analysis
- The Hybrid FePt/FeRh system
- Conclusions

- Sample preparation
-
  -
  -
-
  -
  -
-
-

Sample preparation

Triode sputtering

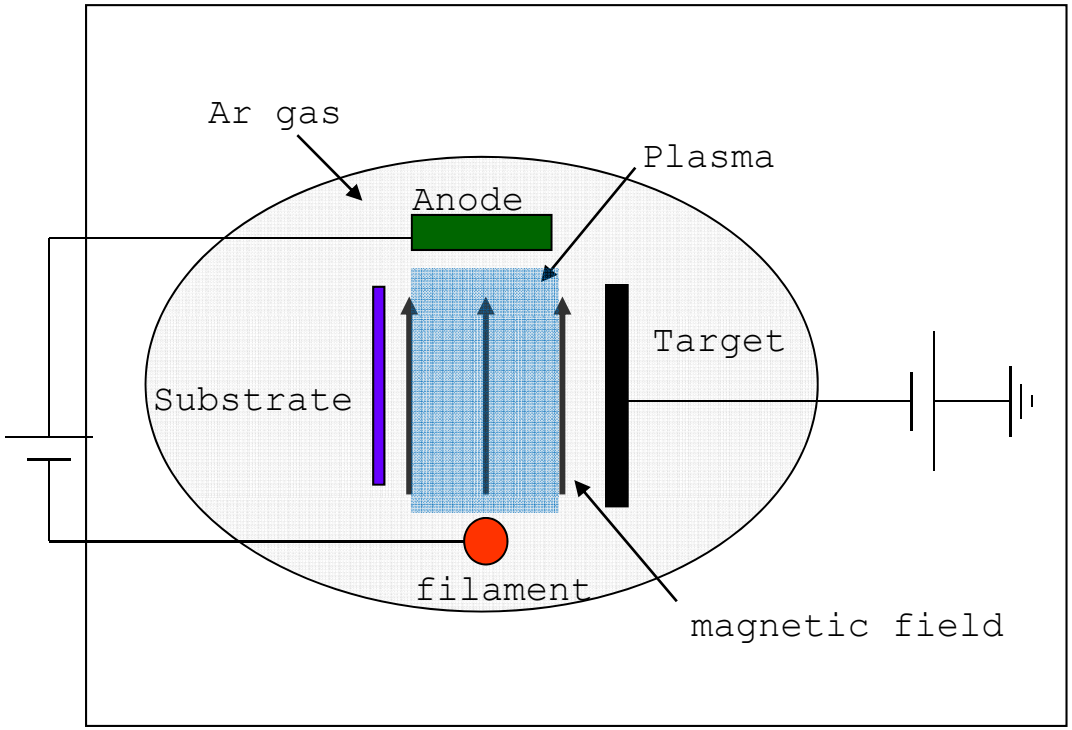

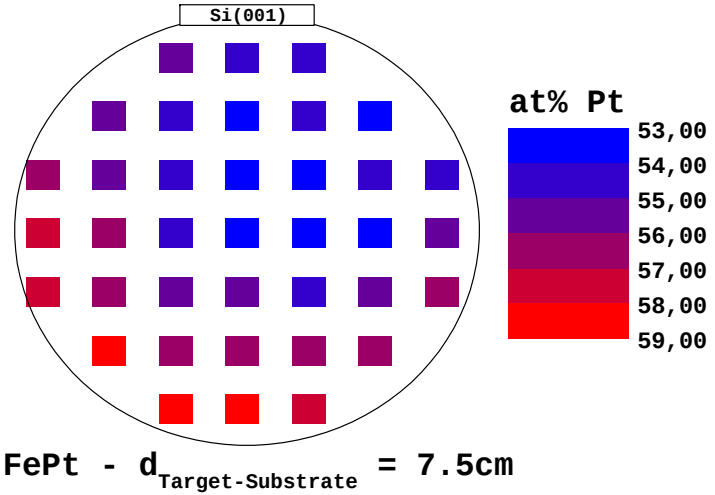

- Base pressure : 2.10^{-6} mbar
- Sputtering pressure : 2.10^{-3} mbar
- Si Substrate (Φ = 100mm)
- Target : -900V

Deposition rate :
~ 0,5 - 1nm/s (2,8µm/h)

High deposition rate over large areas makes this system compatible with MEMS platforms (large substrates…)

- The FePt System

FePt system

Phase Diagram & Crystalline Structures

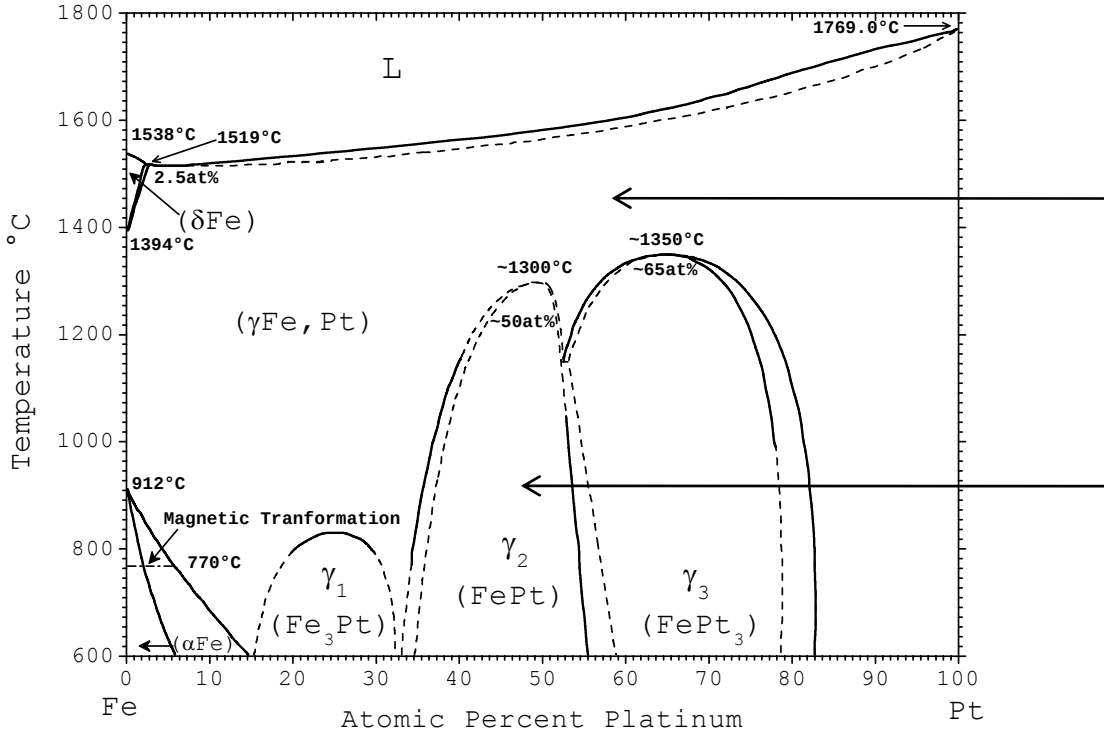

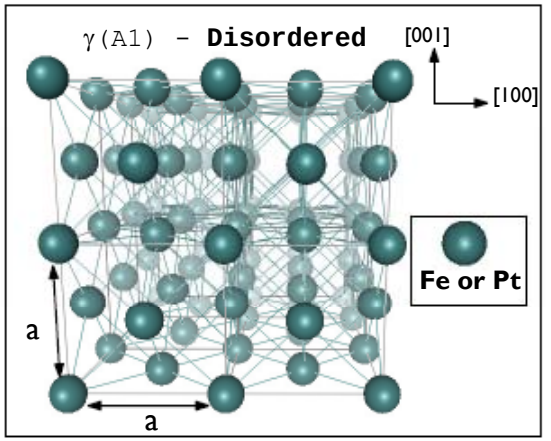

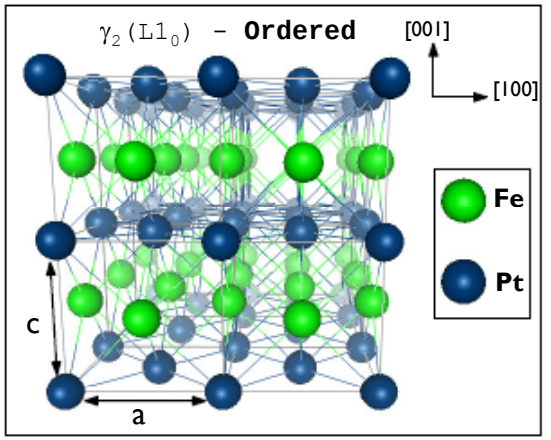

- $\gamma(A1)$: disordered phase - cubic symmetry - low magnetic anisotropy
- $\gamma_2(L1_0)$: ordered phase - tetragonal symmetry - high magnetic anisotropy

- Experimental results
  - Impact of composition on $L1_0$ ordering
  - Effects of adding Cu to FePt system

- Experimental results
  - Impact of composition on $L1_0$ ordering

FePt system:

Impact of composition on $L1_0$ ordering

X-Ray analysis

when Pt content increases:

-The intensity of the superlattice peaks decreases
-The intensity of the fundamental peaks increases

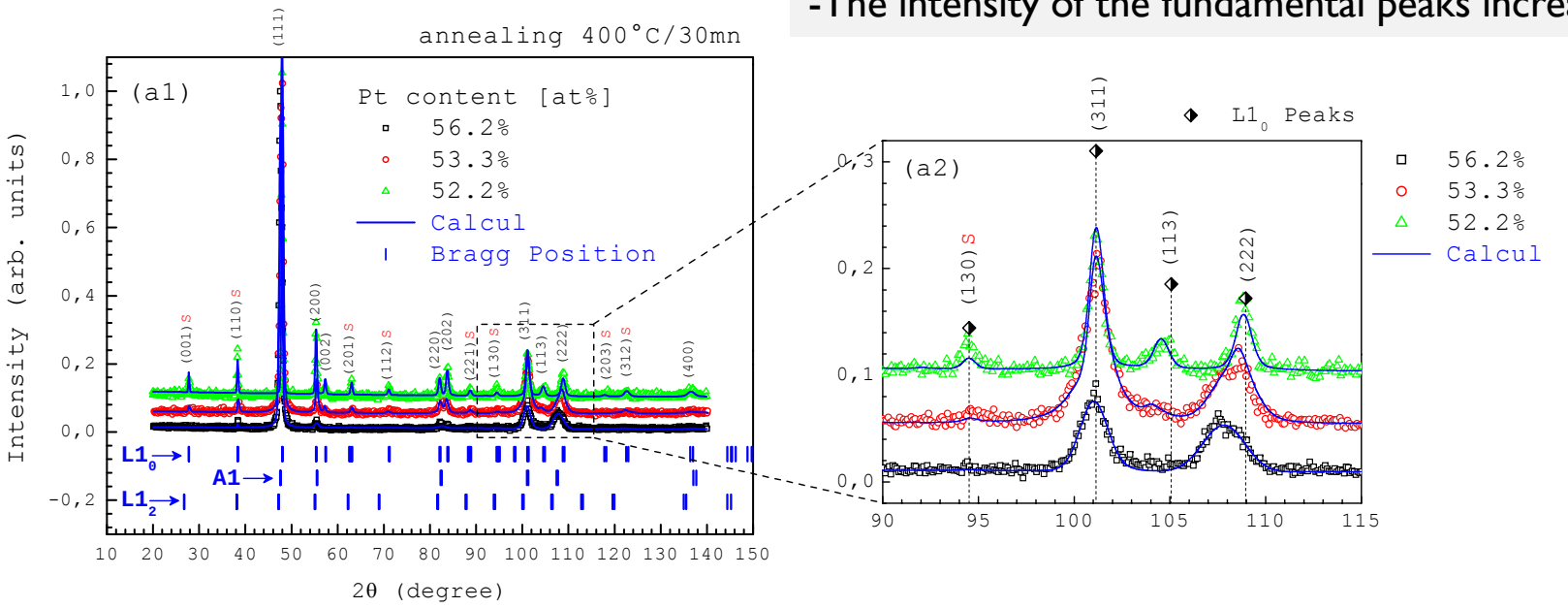

FePt system:

Impact of composition on $L1_0$ ordering

X-Ray analysis

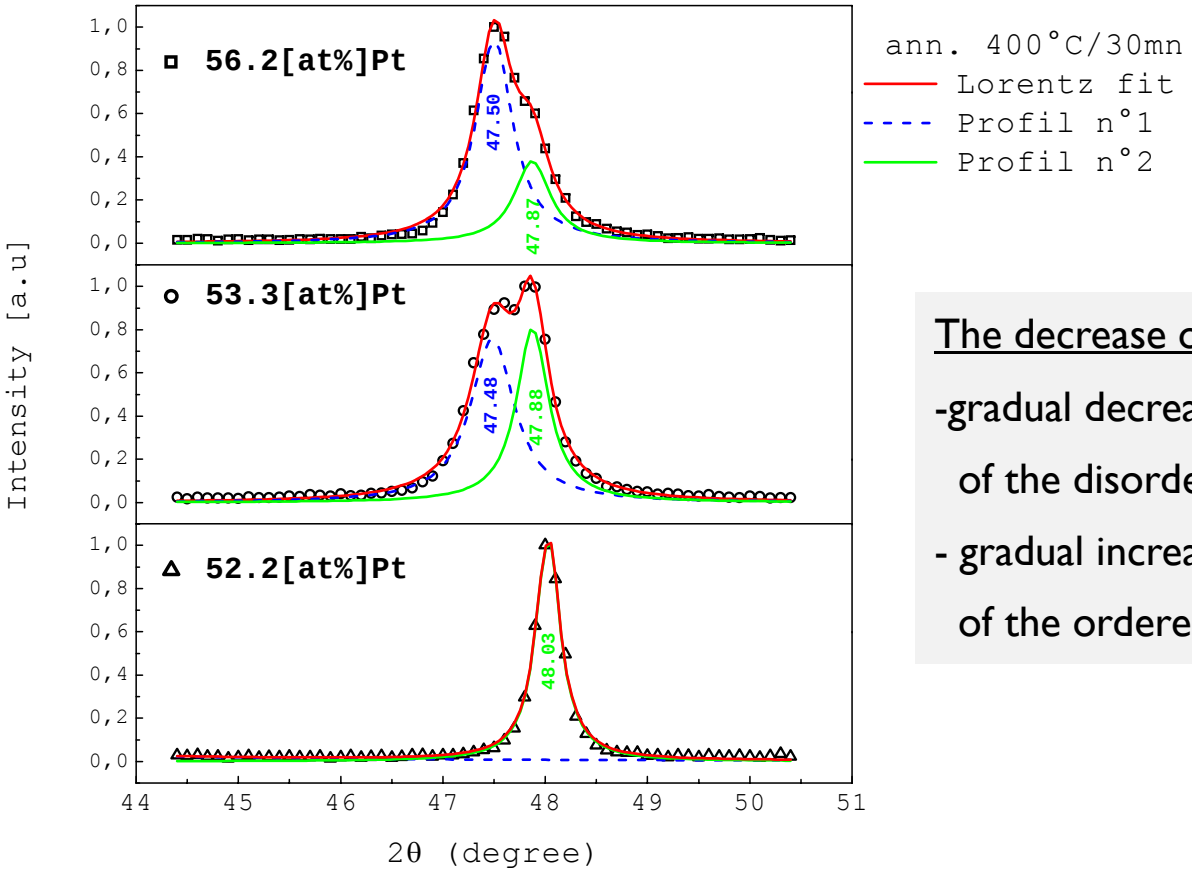

The decrease of Pt content causes:

-gradual decrease of fundamental peaks of the disordered A1 phase

- gradual increase of fundamental peaks of the ordered $L1_0$ phase

FePt system:

Impact of composition on $L1_0$ ordering

Magnetometry analysis

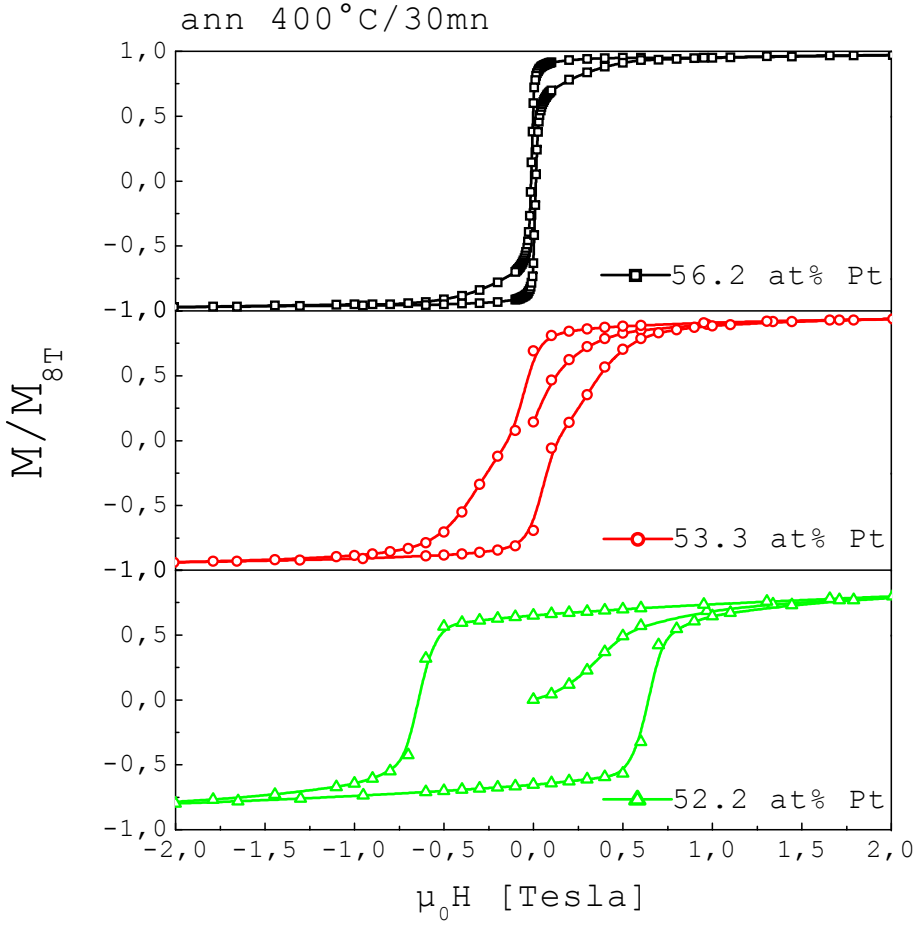

The increase of Pt content causes:

- gradual disappearance of the hard magnetic behaviour associated with the $L1_0$ phase
- gradual increase of the soft phase behaviour associated with the A1 phase

FePt system:

Impact of composition on $L1_0$ ordering

Magnetometry analysis

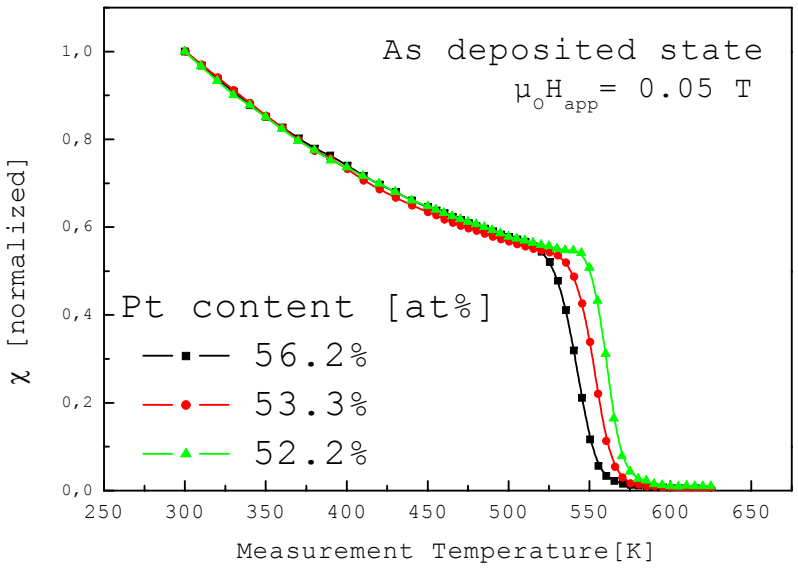

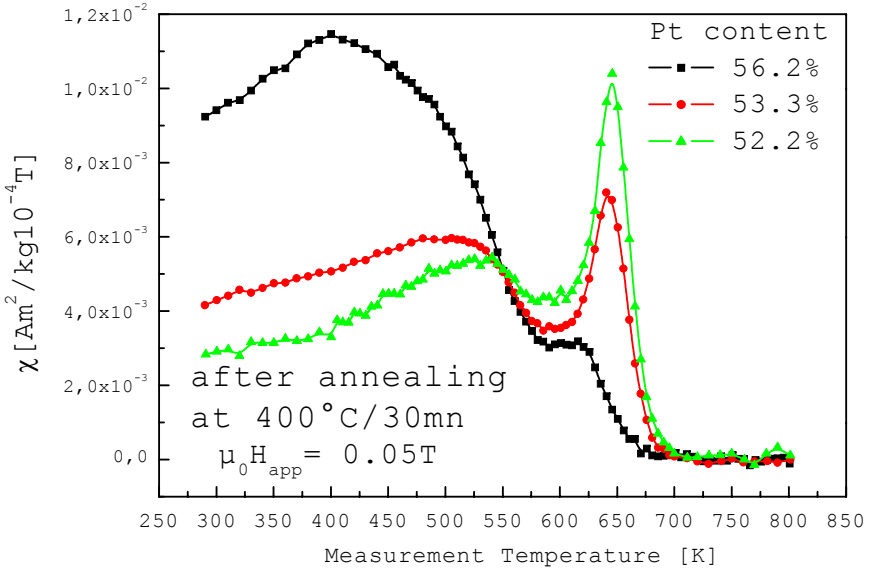

The decrease of the Pt content causes:

- gradual increase of the Curie temperature of both A1 and $L1_0$
- gradual decrease (increase) of the contribution of the A1 ($L1_0$) phase after annealing

FePt system:

Impact of composition on T_c

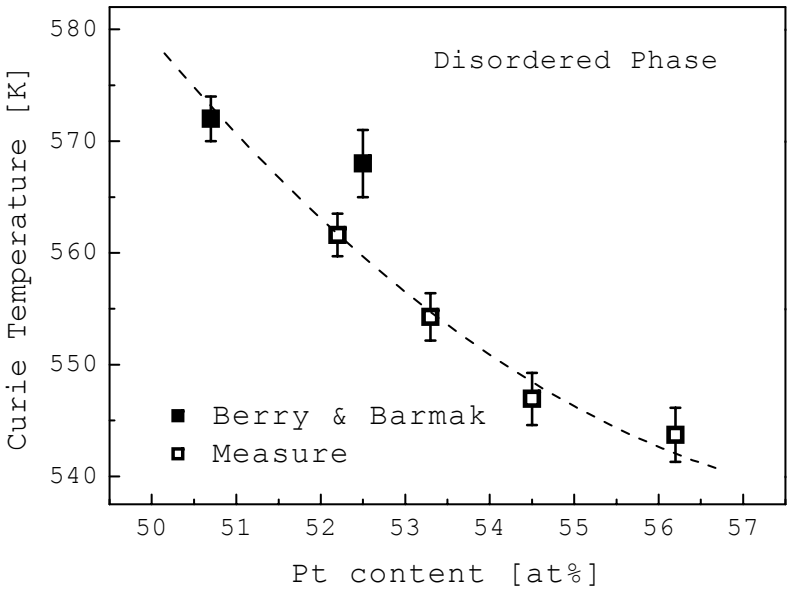

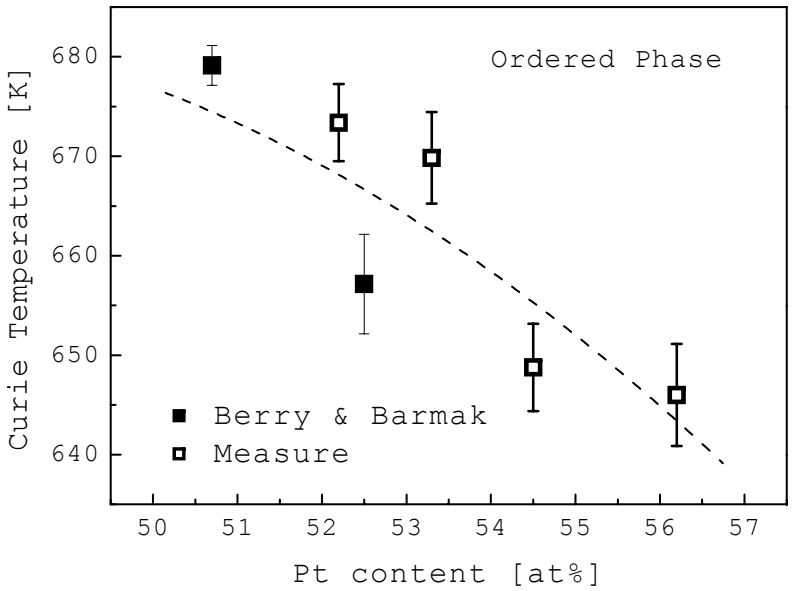

The increase of the Pt content causes a gradual decrease of the Curie temperature in both phases

D. C. Berry et K. Barmak JAP.vol.102.pp024912(2007)

- Experimental results
  - Effects of adding Cu to FePt system

FePt system:

Adding Cu to the FePt system

X-Ray analysis

when Cu content increases:

- The intensity of the superlattice peaks increases
- The different Bragg peaks are not influenced in the same way

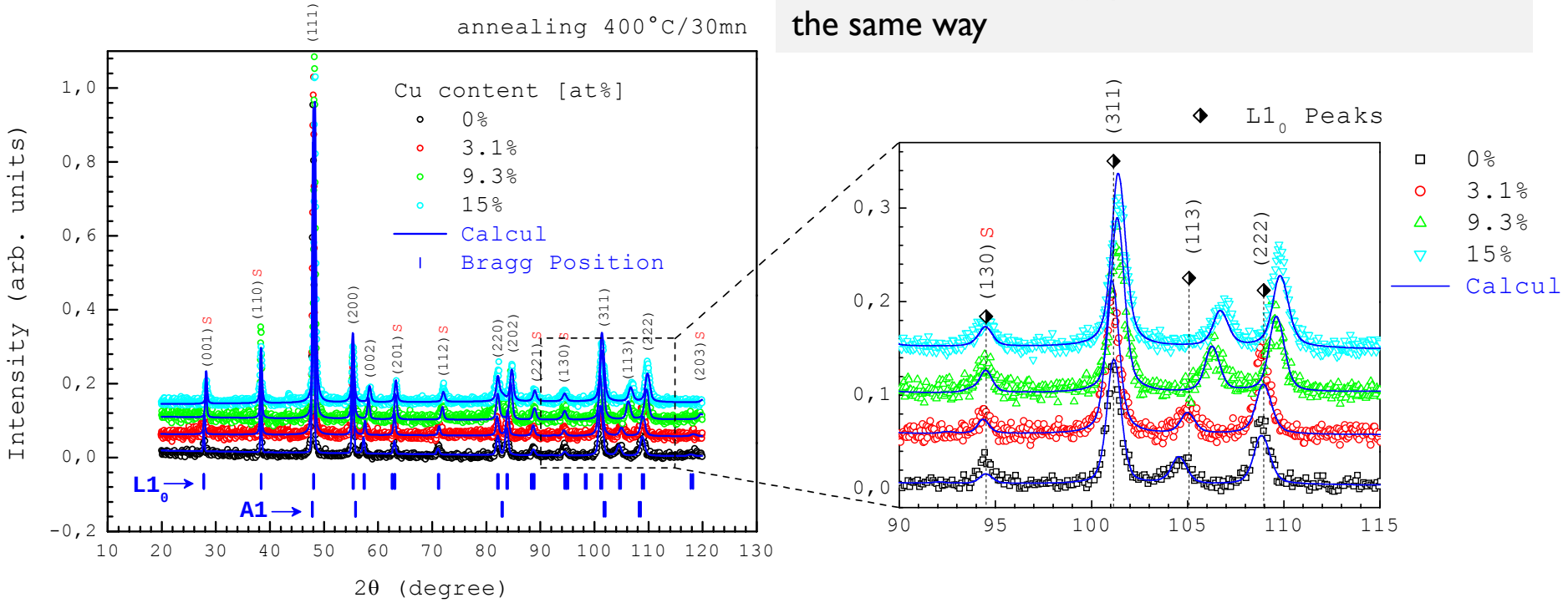

FePt system:

Adding Cu to the FePt system

X-Ray analysis

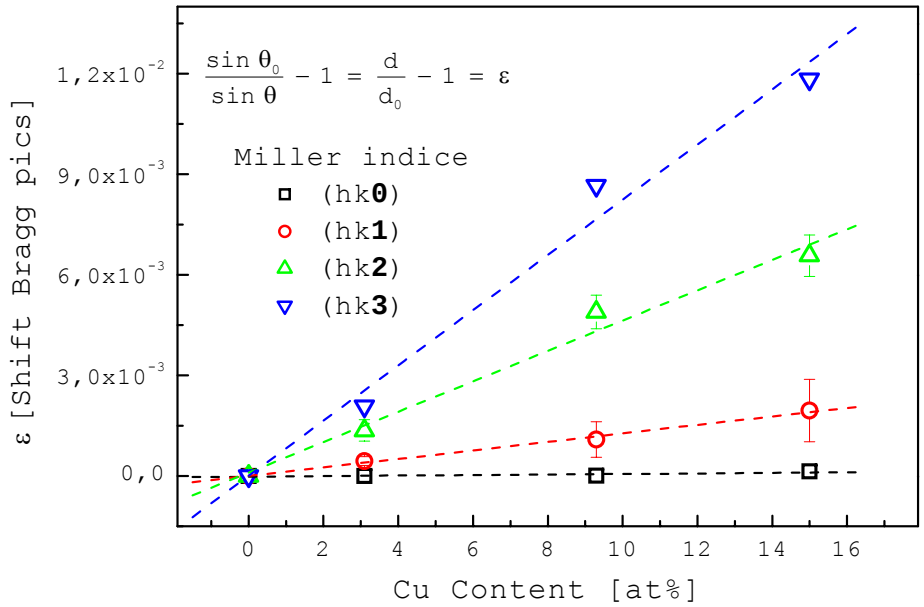

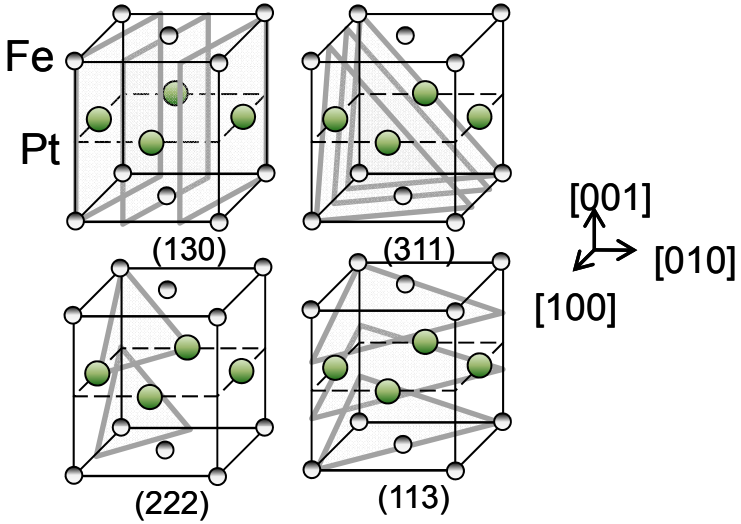

when Cu content increases:

-The shift of the Bragg peaks increases with increasing the value of the last Miller index (ℓ parameter)

- Preferential occupation of Cu on the Fe sites

a(CuPt) (fcc) = 3.796
a(FePt) (fcc) = 3.816

FePt system:

Adding Cu to the FePt system

Susceptibility behaviour near T_C

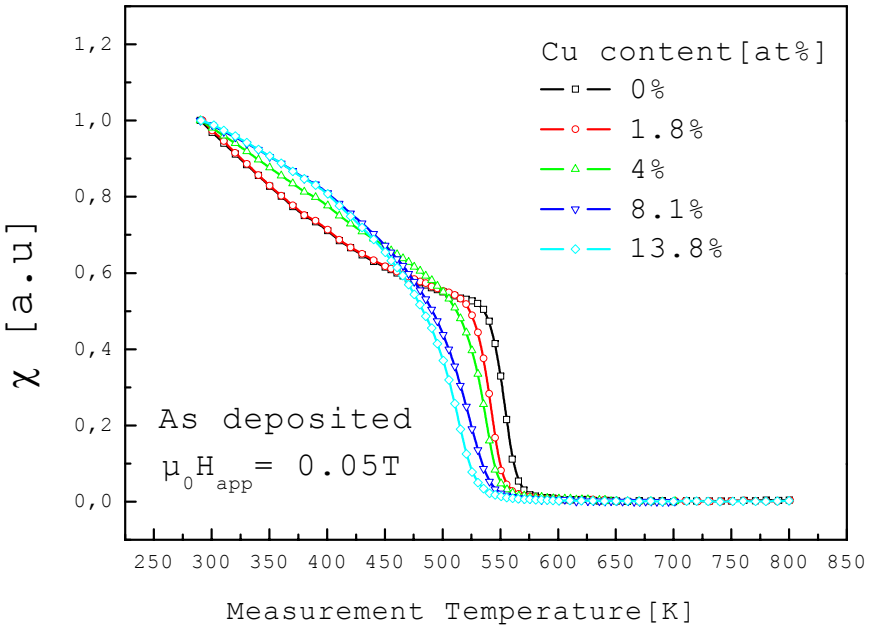

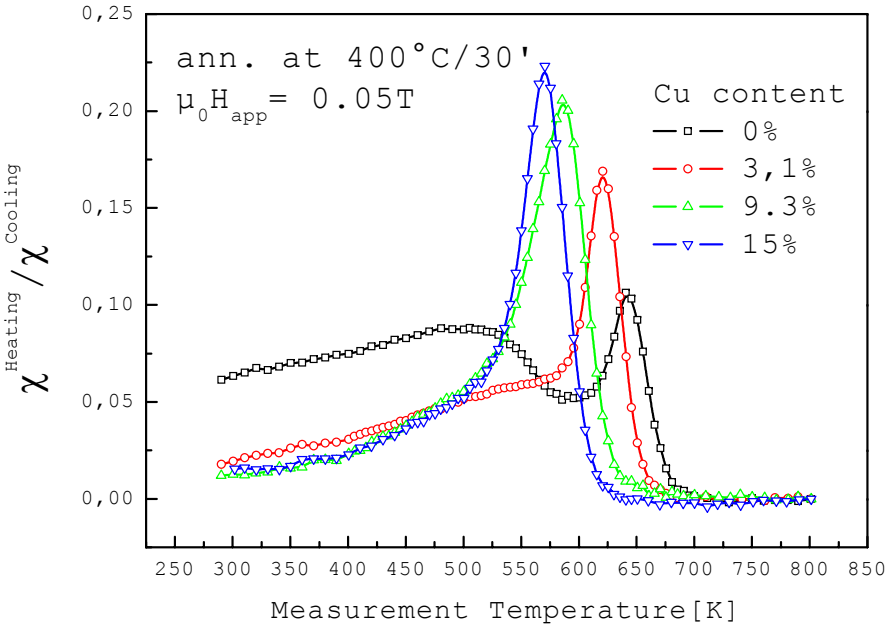

when the Cu content increases:

- The Curie temperature and the discontinuity at the transition decreases in the as deposited state
- Crystallographic ordering is favoured
- Crystallographic ordering of FePt films is accelerated (the ordering temperature is reduced)

FePt system:

Lattice Parameters and Order Parameter

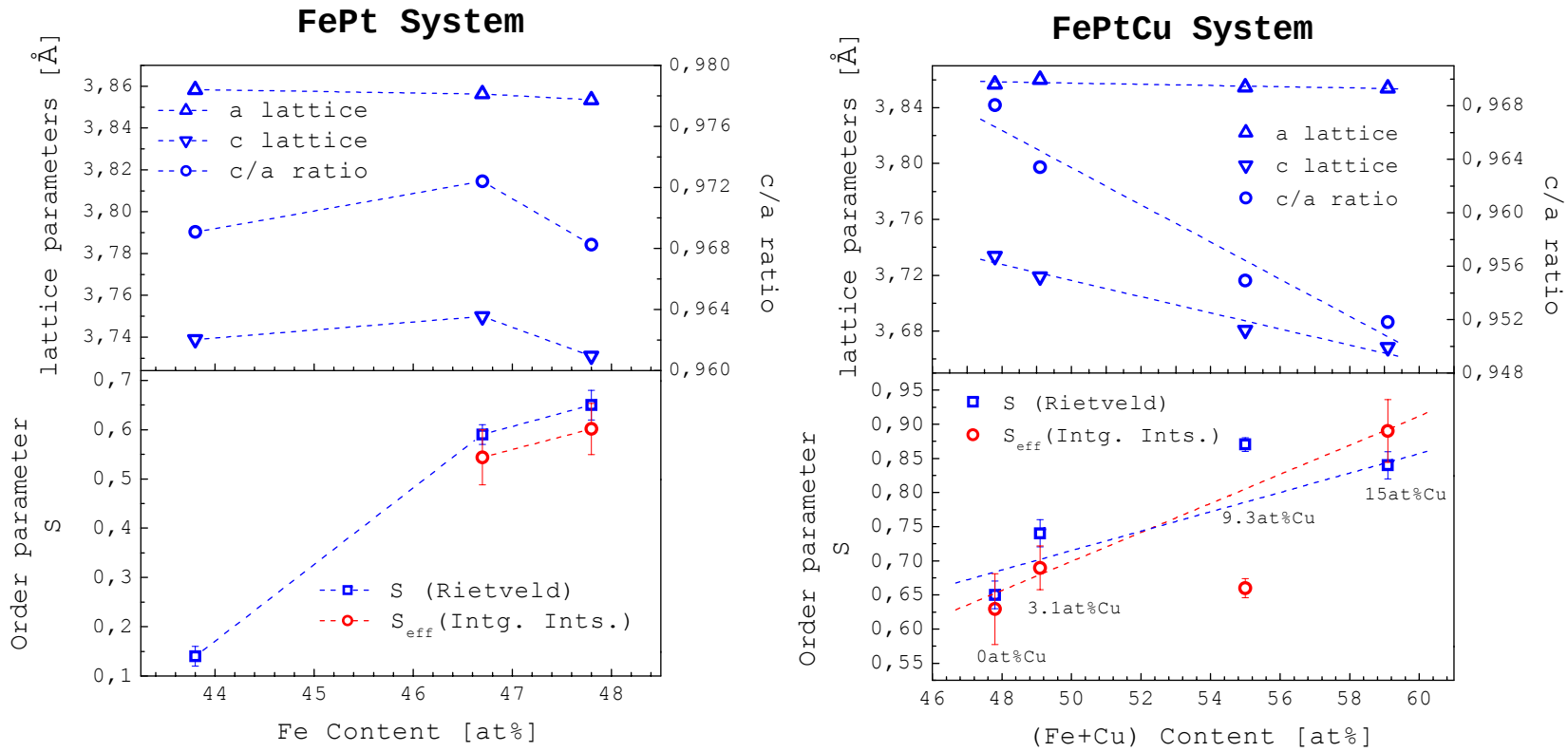

- Continuity of the results of both systems.
- The addition of Cu in the FePt system allows to decrease the Pt content.

-
-
  -
  - Analysis
-
  -
  -
-
-

FePt system:

Model: Presentation

Modeling of magnetization curves in polycrystalline systems

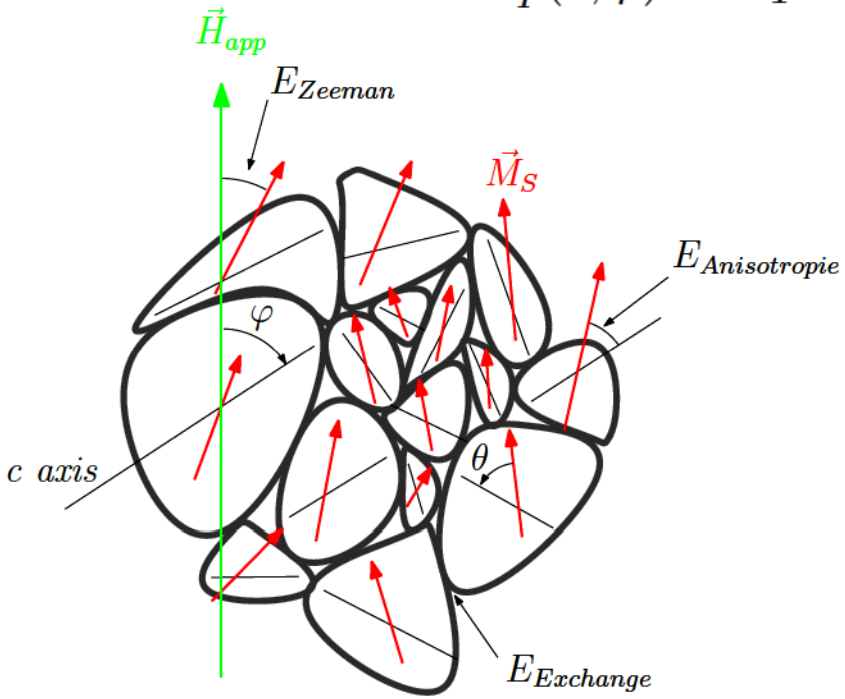

$$E_T(\theta,\varphi) = K_T \sin^2(\theta) - \mu_0 M_S (H_{app} + \underbrace{\eta < M >}_{H_{ex}}) \cos(\varphi - \theta)$$

$$E_A(\theta) = K_T \sin^2(\theta) + \frac{1}{2} N_{\parallel} \mu_0 M_S^2$$

$$E_Z(\varphi,\theta) = -\mu_0 \vec{M}_S \cdot \vec{H}_{app}$$

$$E_{exch}(\varphi,\theta) = -\mu_0 \vec{M}_S \cdot \vec{H}_{ex}$$

- Crystallites randomly distributed
- Single domain particles
- Assembly of exchange coupled crystallites

FePt system:

Model: Presentation

Approximation of reversible rotation of magnetization in polycrystalline systems

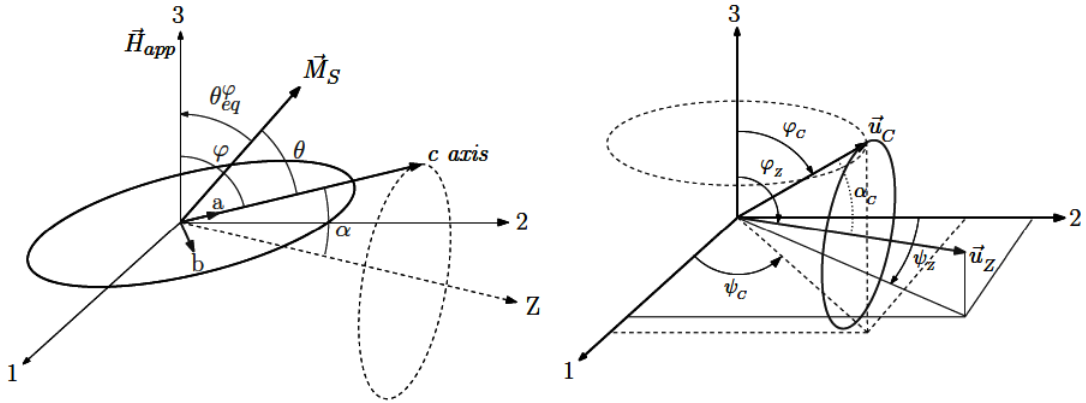

$$E_T(\theta,\varphi) = K_T \sin^2(\theta) - \mu_0 M_S (H_{app} + \eta < M >) \cos(\varphi - \theta)$$

$$< M >= \frac{\sum_{\varphi_C} \sum_{\psi_C} M_S \cos\theta_{eq}^{\varphi_C} \cdot \sin\varphi_C D_o\left[\alpha_C\left(\varphi_C,\psi_C\right)\right]}{\sum_{\varphi_C} \sum_{\psi_C} \sin\varphi_C D_o\left[\alpha_C\left(\varphi_C,\psi_C\right)\right]}$$

$$D_o(\alpha_C) = \frac{1}{\sigma\sqrt{2\pi}} e^{-\frac{\alpha_C^2}{2\sigma^2}}$$

$$\alpha_C\left(\varphi_C,\psi_C\right) = arccos\left\{\sin\varphi_z \sin\varphi_C \left[\sin\left(\psi_C + \psi_z\right)\right] + \cos\varphi_z \cos\varphi_C\right\}$$

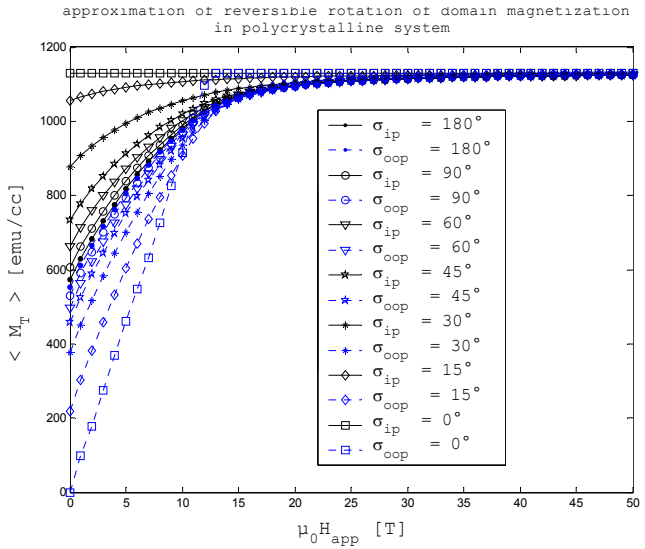

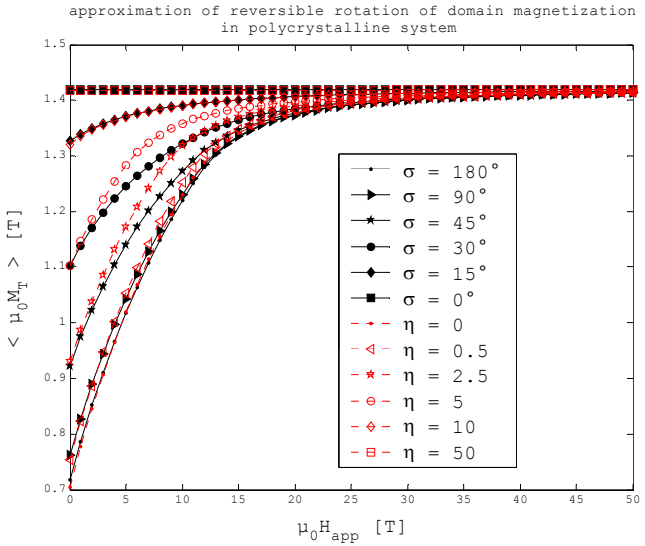

FePt system:

Model: Presentation

Approximation of reversible rotation of magnetization in polycrystalline systems

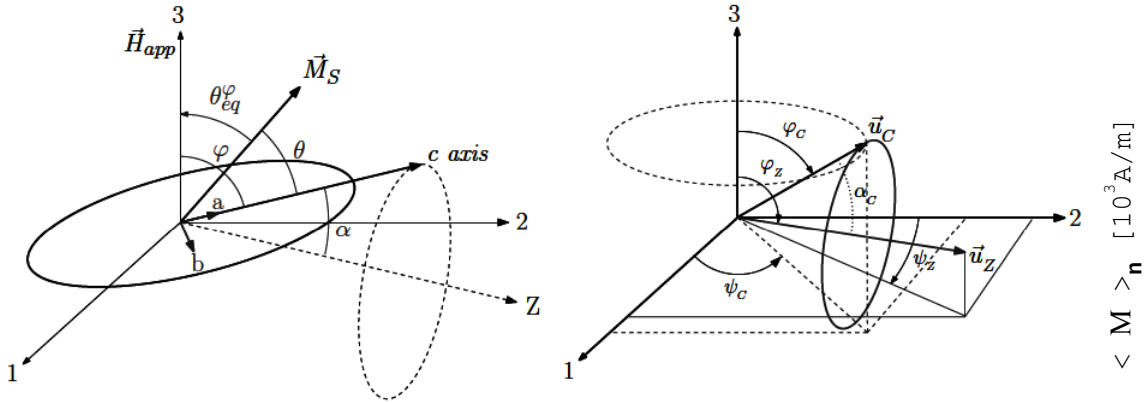

$$E_T(\theta,\varphi) = K_T \sin^2(\theta) - \mu_0 M_S (H_{app} + \eta < M >) \cos(\varphi - \theta)$$

$$< M >= \frac{\sum_{\varphi_C} \sum_{\psi_C} M_S \cos\theta_{eq}^{\varphi_C} \cdot \sin\varphi_C D_o\left[\alpha_C\left(\varphi_C,\psi_C\right)\right]}{\sum_{\varphi_C} \sum_{\psi_C} \sin\varphi_C D_o\left[\alpha_C\left(\varphi_C,\psi_C\right)\right]}$$

$$D_o(\alpha_C) = \frac{1}{\sigma\sqrt{2\pi}} e^{-\frac{\alpha_C^2}{2\sigma^2}}$$

$$\alpha_C\left(\varphi_C,\psi_C\right) = arccos\left\{\sin\varphi_z \sin\varphi_C \left[\sin\left(\psi_C + \psi_z\right)\right] + \cos\varphi_z \cos\varphi_C\right\}$$

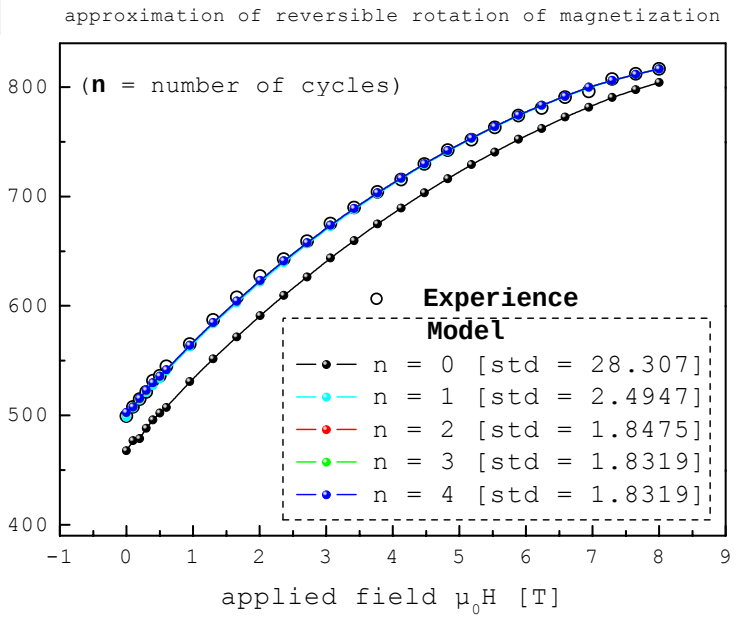

Std: standard deviation

FePt system:

Model vs Measurement

Modeling of magnetization curves

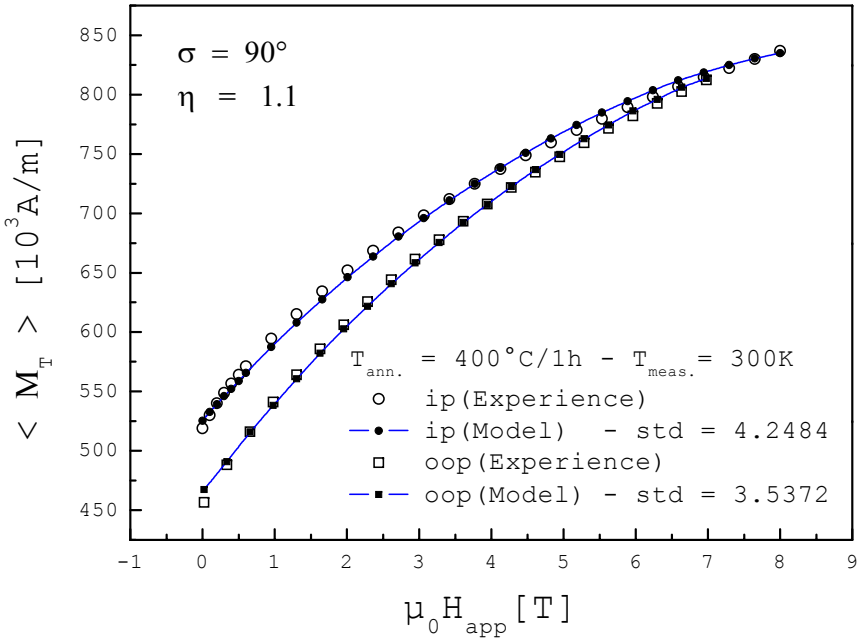

The η (intergranular coupling) and σ (texture) parameters are fixed by fitting the experimental results in both directions of applied field

FePt system:

Model vs Measurement

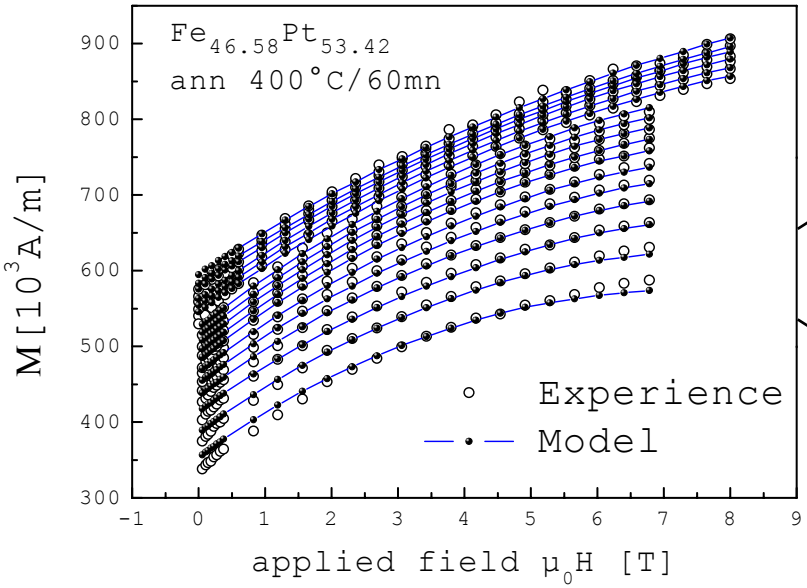

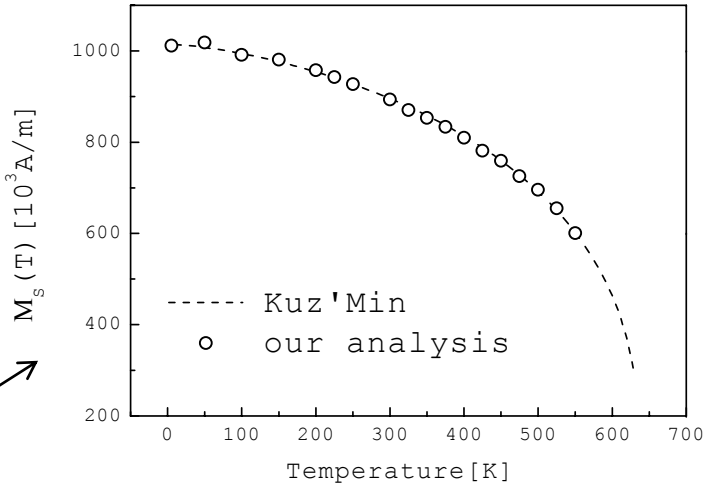

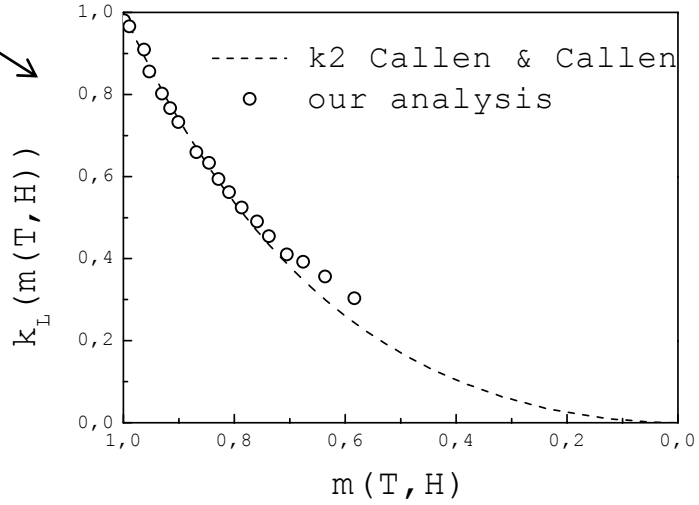

M_S and K_T extracted at each temperature and compared to the theoretical models proposed respectively by Kuzmin[1] and Callen & Callen[2]

[1]Kuz'min Phys. Rev. Lett.,94.107204 (2005)
[2]H.B. Callen and E. Callen, J. Phys. Chem. Solids 27, 1271 (1966)

FePt system:

Model vs Measurement

Determination of the anisotropy field

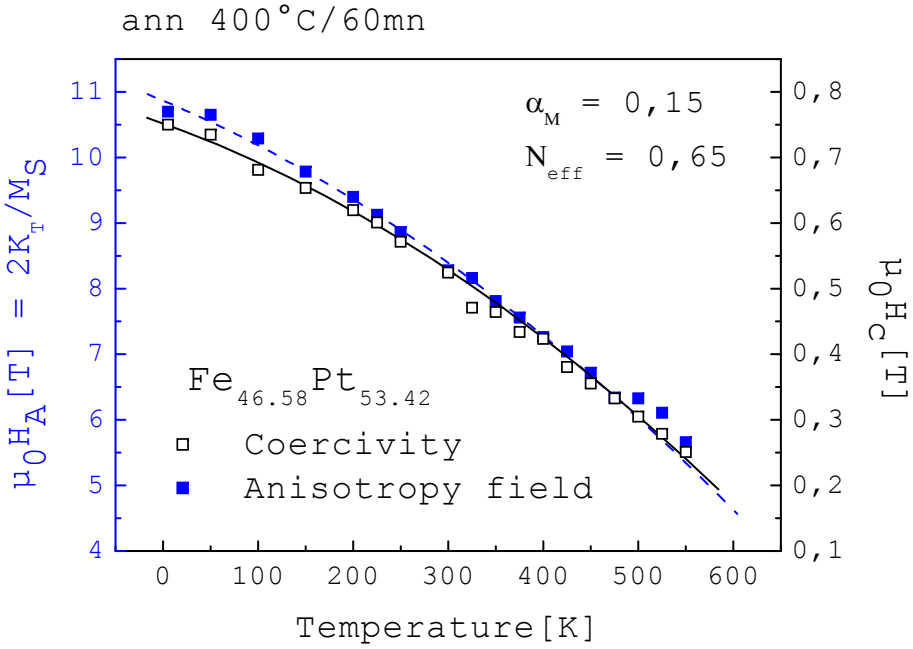

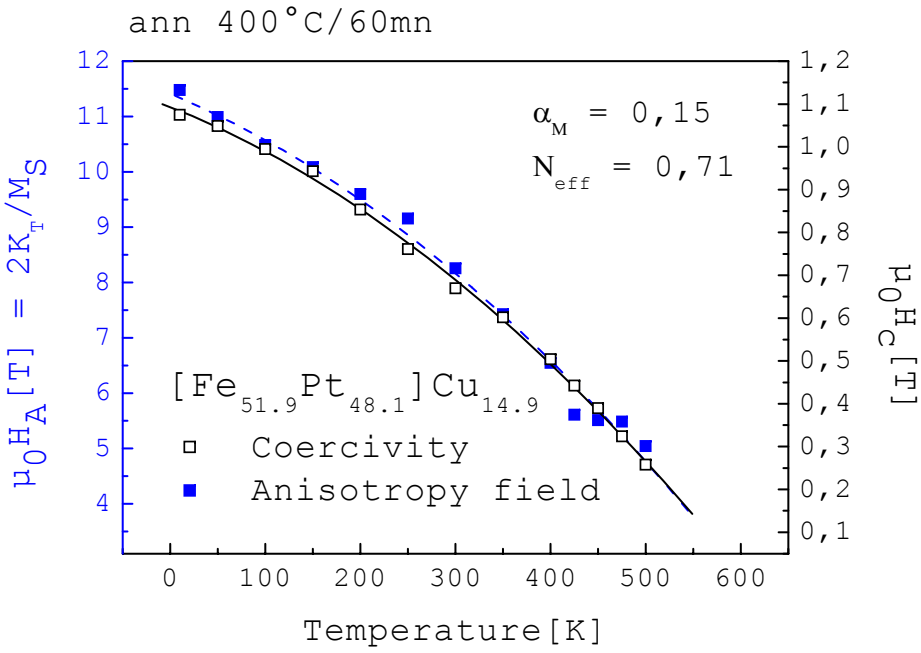

The micromagnetic model[1] enables one to quantify the reduction parameter (α_M) of the anisotropy field and the effect of the dipolar interactions (N_{eff})

$$\mu_0 H_C = \alpha_M \mu_0 H_A - \mu_0 N_{eff} M_S$$

[1]Kronmüller et al. JMMM.Vol.74.pp291-302 (1988)

FePt system:

Model vs Measurement

Hopkinson peak: Modelization of the demagnetized state

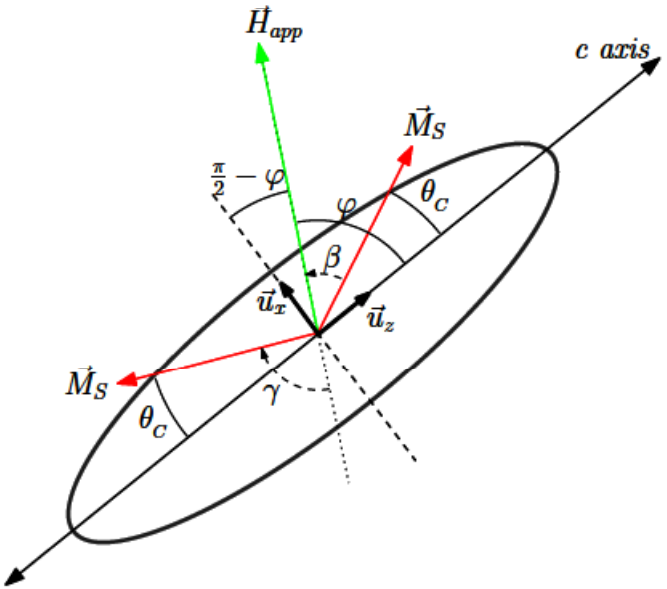

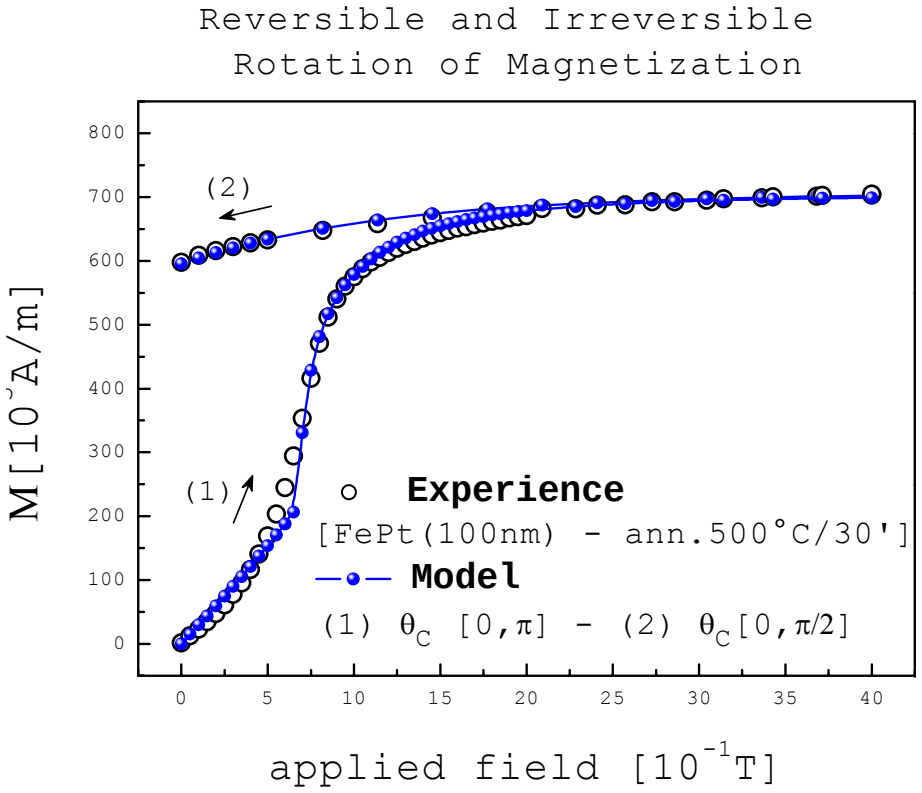

- The reversible magnetization process occurs if $|\varphi - \theta_c| < \pi/2$
- The irreversible magnetization process occurs if $|\varphi - \theta_c| > \pi/2$

FePt system:

Model vs Measurement

Hopkinson peak: Modelization of the demagnetized state

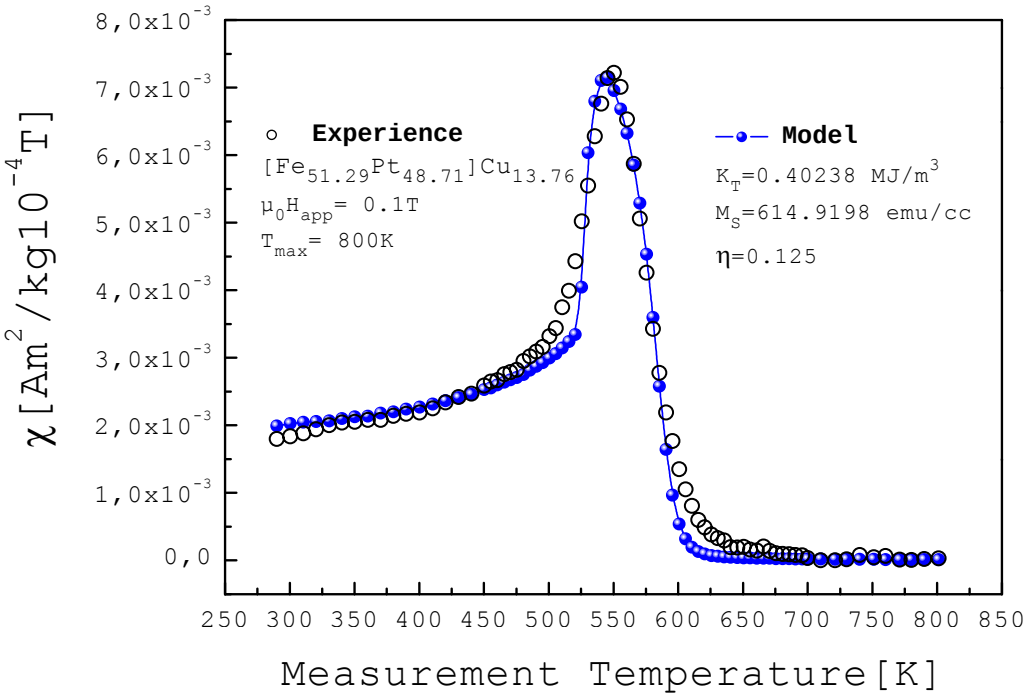

Origin:

The Hopkinson peak is related to the magnetization process of the $L1_0$ phase and comes from the irreversible rotation of magnetization

Beyond permanent magnets: switchable magnetic materials

- Why go beyond hard magnets?

  The interaction current-field is driven by currents in coils
  - Joule heating losses
  - Complex design

- Switchable magnetic materials:

  Reversible change of magnetic properties (M_S, H_A) by an external parameter.

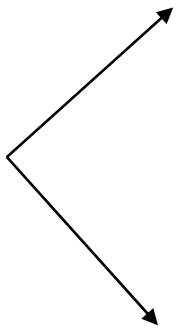

E-field switchable

Modification of intrinsic properties.

e.g. $\mathbf{H_A}$

Thermo-switchable

Modification of magnetic order

e.g. **Ferro ⇔ Para**

or Antiferro ⇔ Ferro

- The FeRh System

FeRh system

Phase Diagram & Crystal Structures

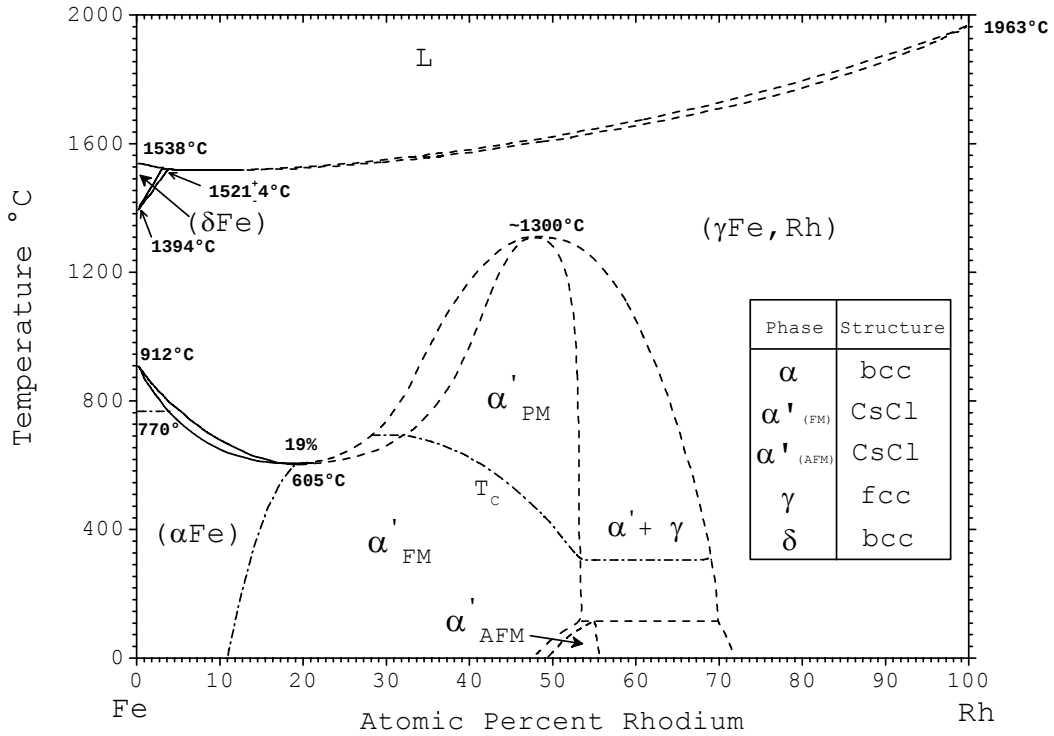

- γ : disordered phase – fcc structure (A1 type) - paramagnetic

- α' : ordered phase – CsCl structure (B2 type) - antiferromagnetic/ferromagnetic

FeRh system

Structural and Magnetic properties

Neutron diffraction[1] performed on a bulk sample with 53[at%] of Rh

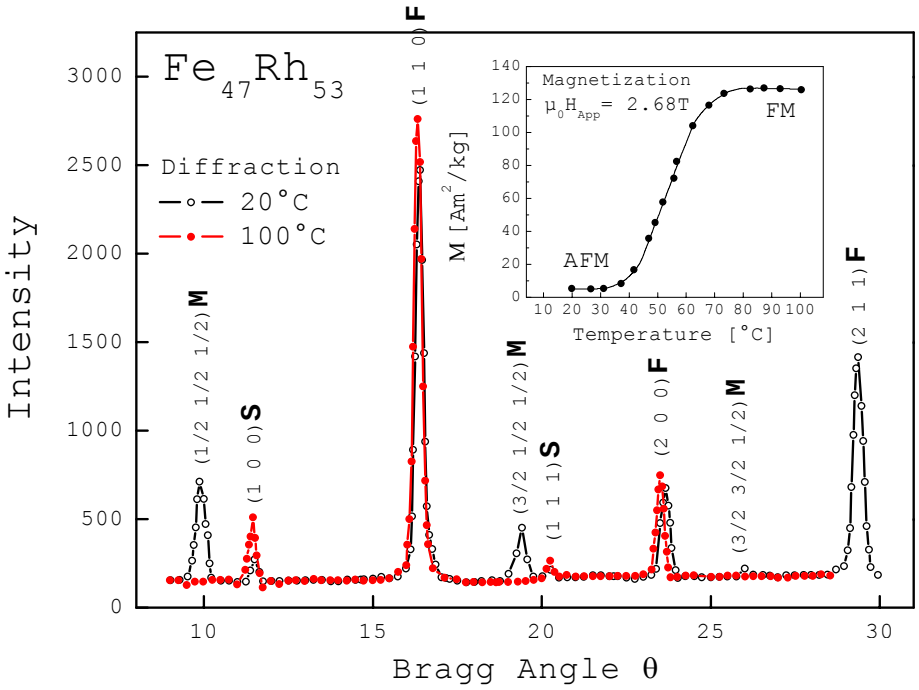

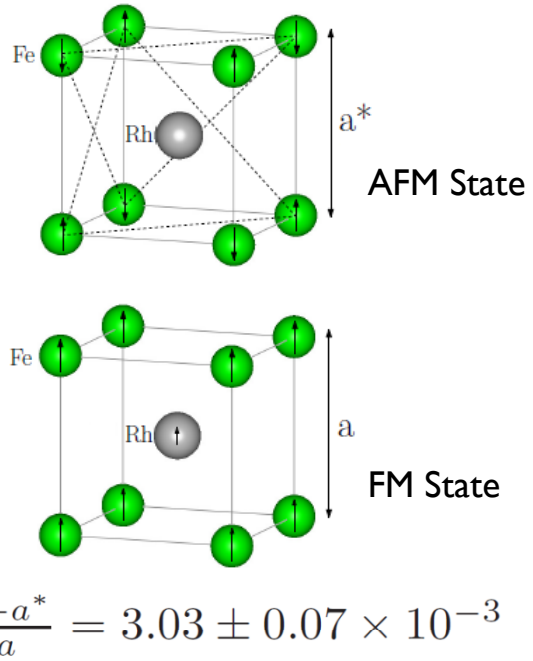

$$\frac{a-a^*}{a} = 3.03 \pm 0.07 \times 10^{-3}$$

- at 20°C: presence of magnetic coherent reflection with Q=π/a(111) -- M ≅ 0 Am² / kg
- at 100°C: only the superstructure and fundamental peaks are present -- M ≅ 125 Am² / kg

[1]F. Bertaut, F. De Bergevin and G. Roult ,C. R. Acad. Sci., 256(8):1688, 1963.

- Experimental results
  - Impact of composition on transition
  - Effects of thermal treatments

- Experimental results
  - Impact of composition on transition

FeRh system

Impact of Rh [at%] on AFM→FM transition

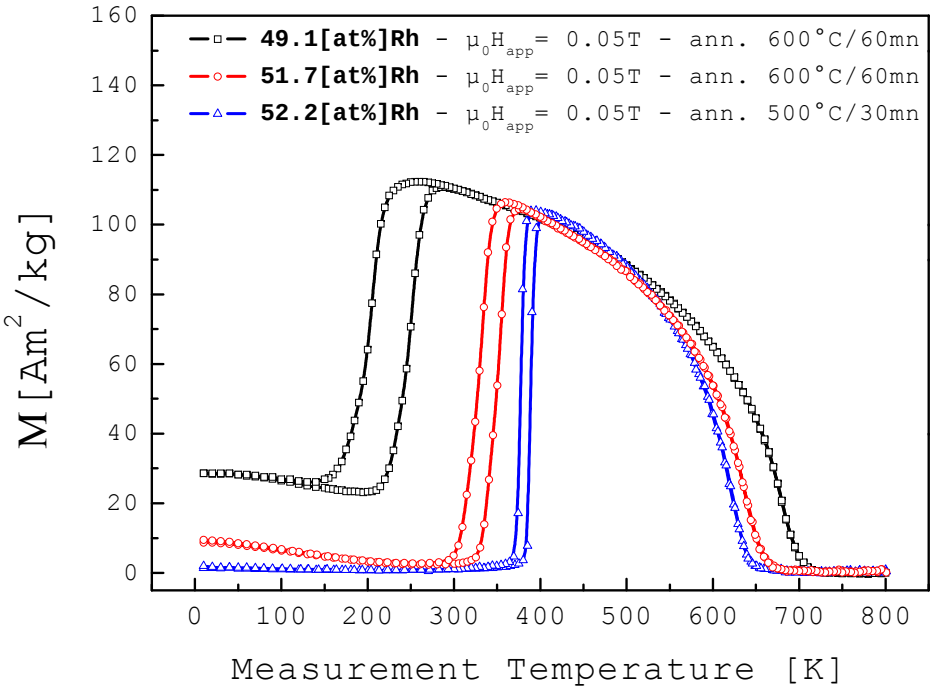

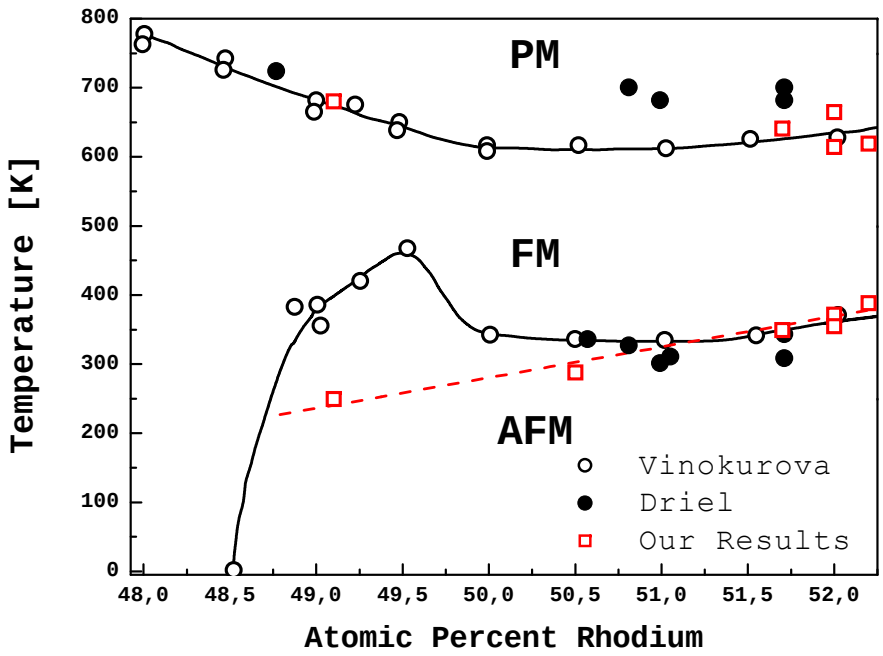

when Rh content increases:

-The Curie temperature decreases

- The transition temperature increases

-The magnetization at low temperature decreases

- The width of thermal hysteresis decreases

} Favours the AFM state

FeRh system

Impact of Rh [at%] on AFM→FM transition

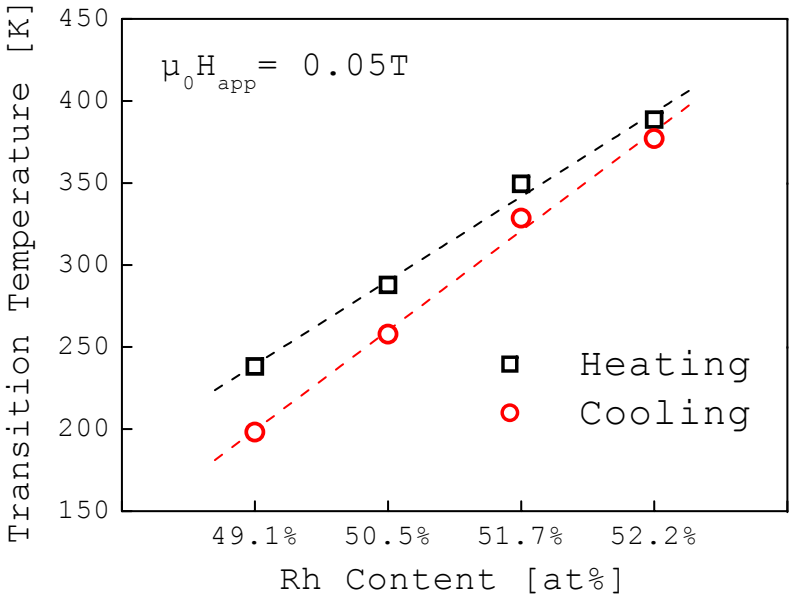

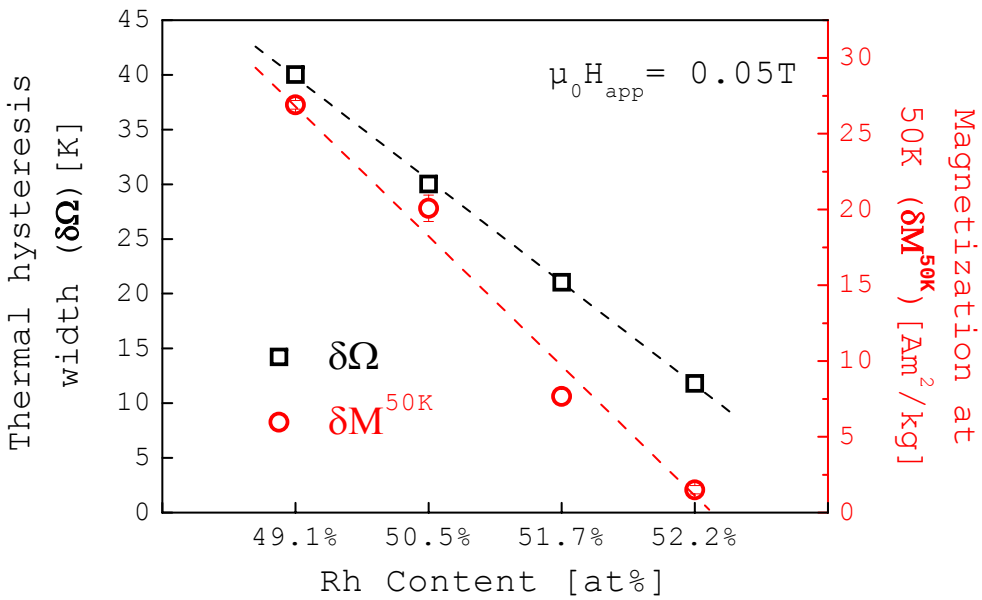

-The variation of the width of thermal hysteresis is correlated with the thermal activation

- The increase of magnetization at low temperature is correlated with the Fe anti-site atoms

- Experimental results
  - Effects of thermal treatments

FeRh system

Effect of thermal treatments

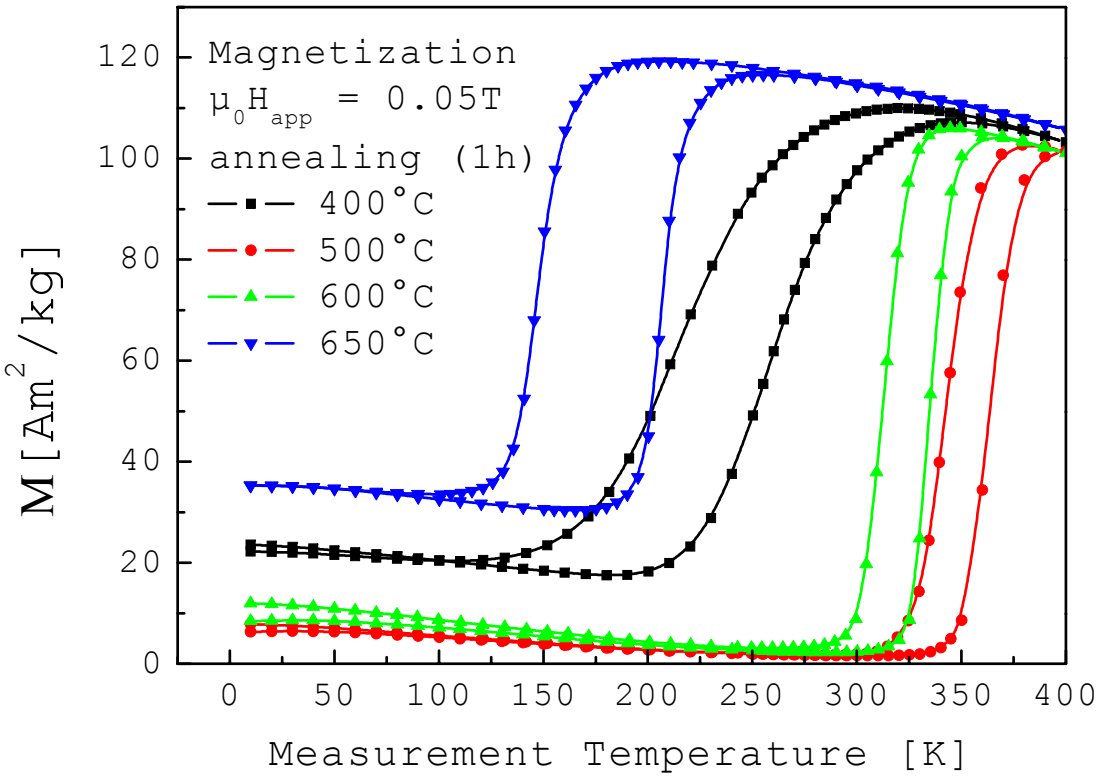

The heat treatments performed on the same sample cause:

- shift of the transition temperature
- variation of the width of thermal hysteresis
- variation of the magnetization at low temperature

FeRh system

Effect of thermal treatments

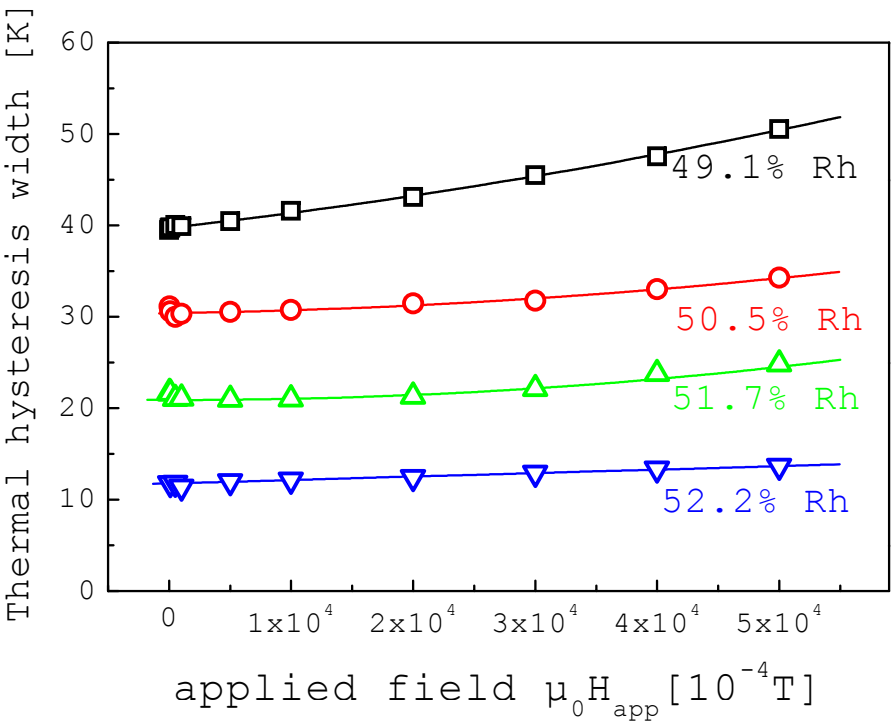

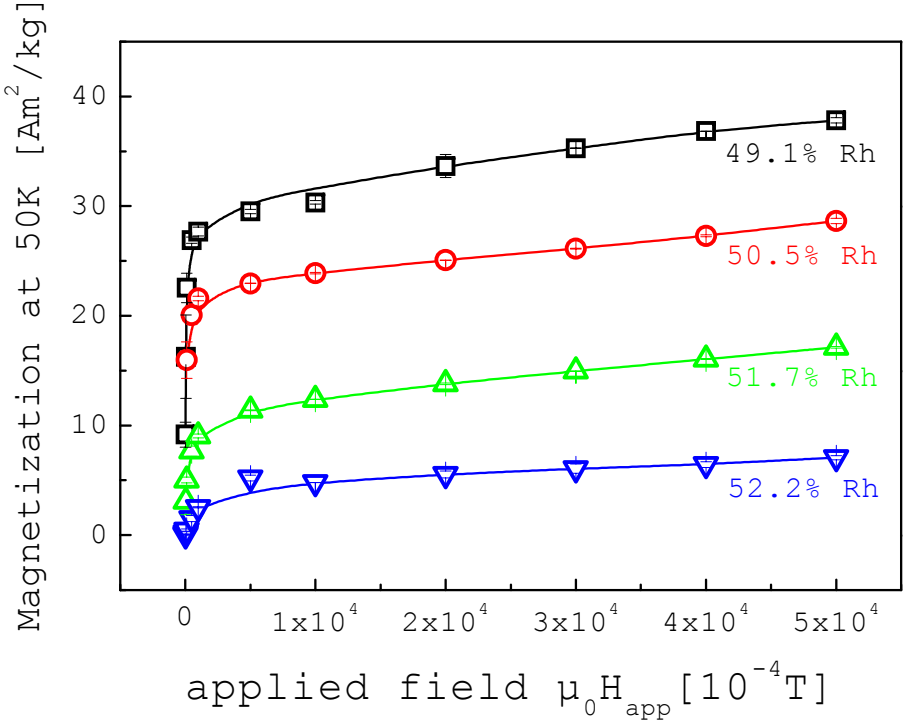

The heat treatment performed on the same sample creates a fluctuation of composition

FeRh system

Effect of thermal treatments

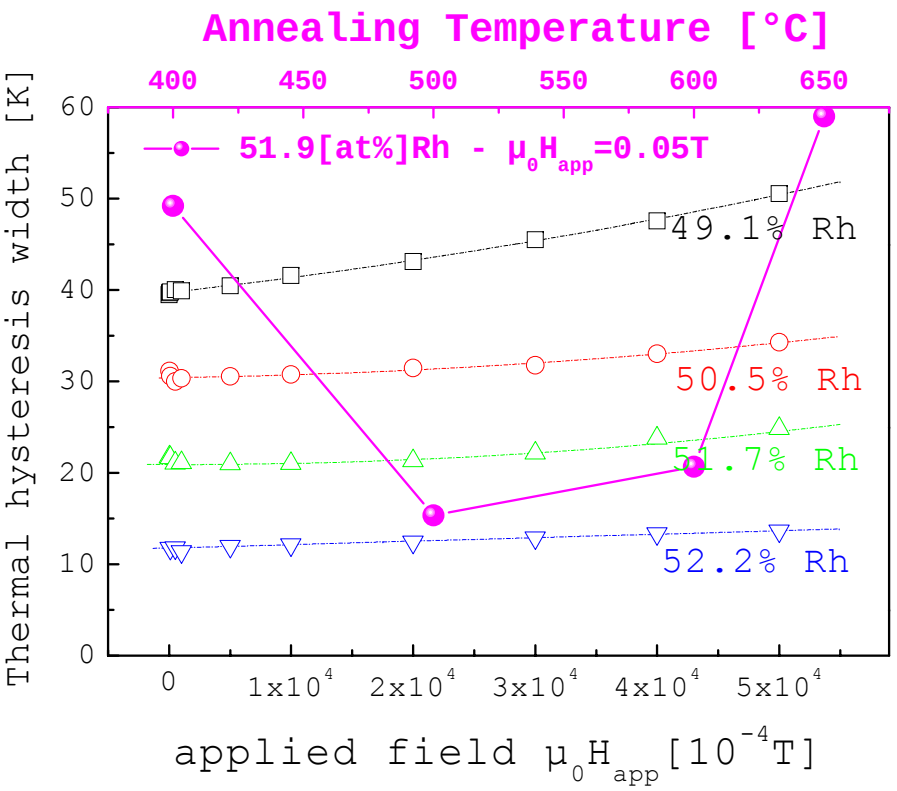

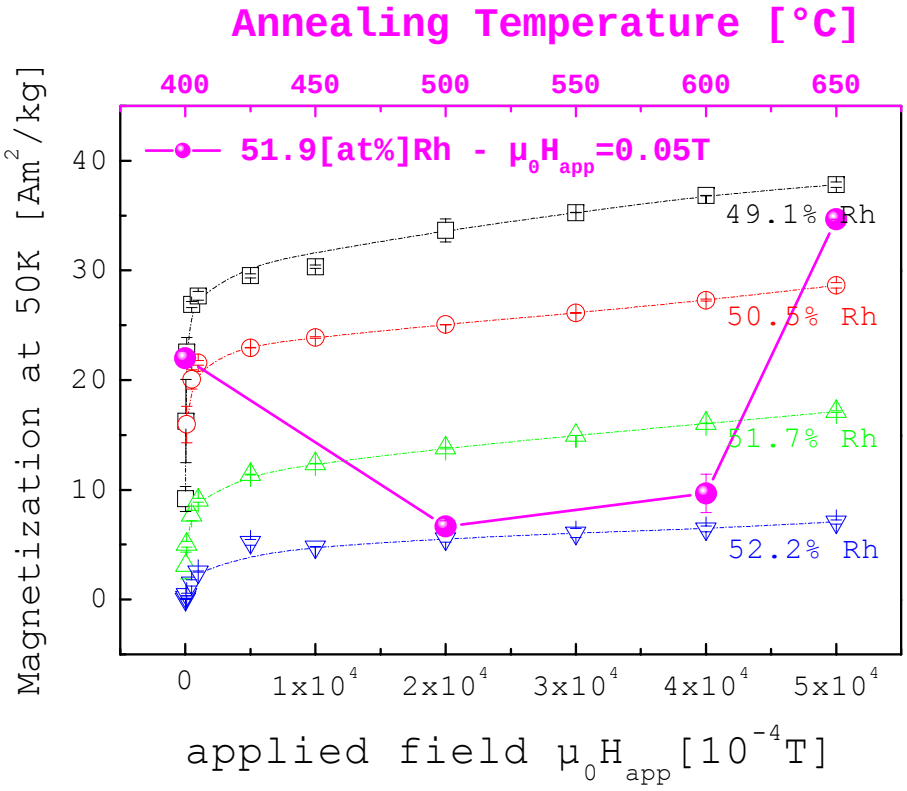

The heat treatment performed on the same sample creates a fluctuation of composition

-
-
  -
  -
-
  -
  - Analysis
-
-

FeRh system

DSC (Differential Scanning Calorimetry) analysis

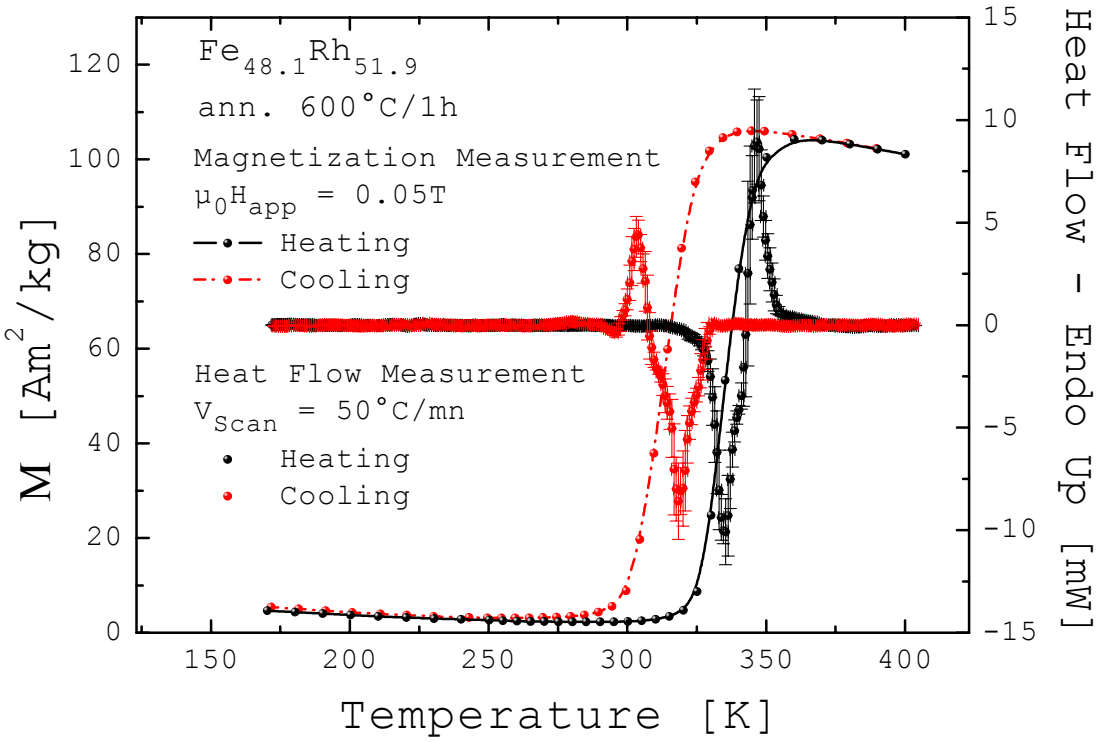

The DSC allows the characterization of the endothermic and exothermic reactions that occur during the transition

$$S_{tot}(T,H) = S_M(T,H) + S_{L+E}(T,H)$$

$$\Delta S_{tot}(T,H) = 0 \Longleftrightarrow \Delta S_M(T,H) = -\Delta S_{L+E}(T,H)$$

FeRh system

DSC (Differential Scanning Calorimetry) analysis

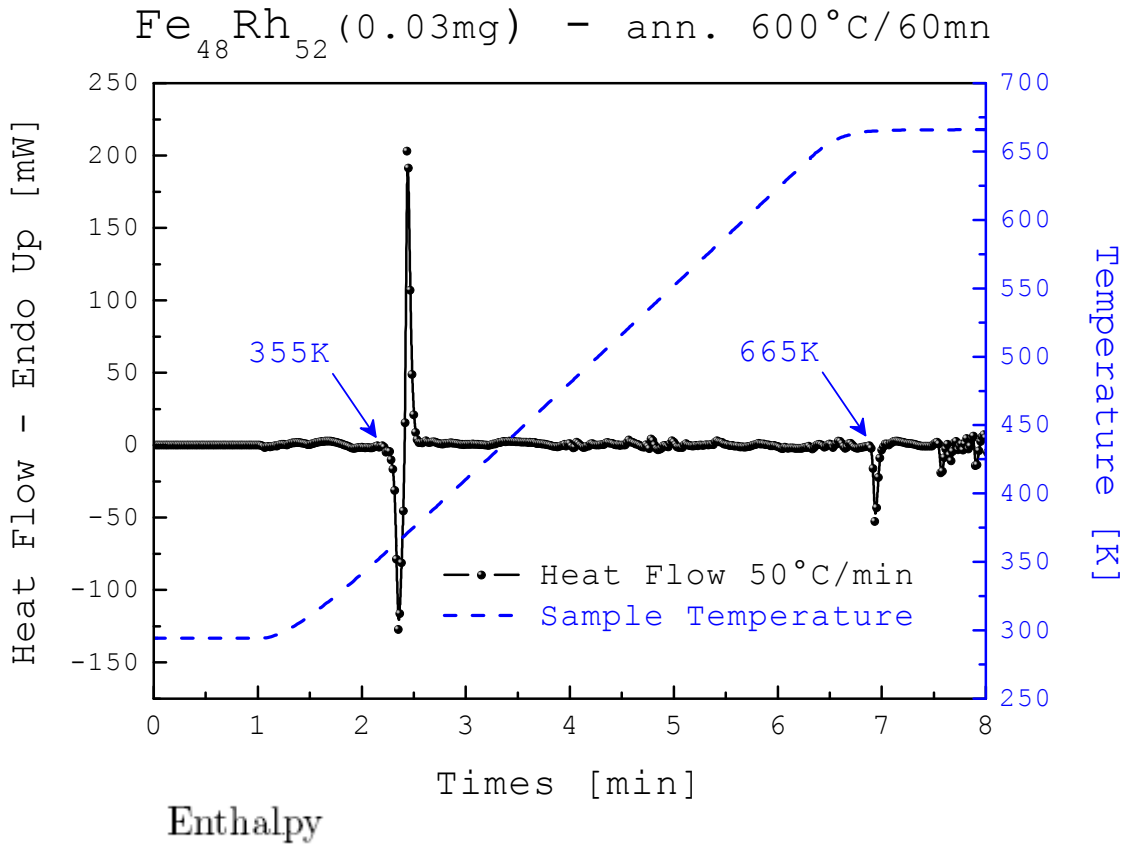

AFM→FM transition:

exothermic + endothermic reactions

FM→PM transition:

exothermic reaction (four times less significant)

Enthalpy

$$\Delta \breve{H}_{AFM\to FM}(exo) = 21.7\mathrm{kJ/g}$$
$$\Delta \breve{H}_{AFM\to FM}(endo) = 22.6\mathrm{kJ/g}$$
$$\Delta \breve{H}_{FM\to PM}(exo) = 5.5\mathrm{kJ/g}$$

FeRh system

DSC vs Magnetic Measurements

$$\left(\frac{\partial S}{\partial H}\right)_{T,P} = -\left(\frac{\partial}{\partial T}\left(\frac{\partial G}{\partial H}\right)_{T,P}\right)_{H,P} = +\left(\frac{\partial M}{\partial T}\right)_{H,P}$$

$$\Longrightarrow \quad \frac{\Delta S_M}{\Delta H} = +\left(\frac{\partial M}{\partial T}\right)$$

$$dS_M(T,H) = \left(\frac{\partial S_M}{\partial T}\right)_H dT + \left(\frac{\partial S_M}{\partial H}\right)_T dH$$

$$dS_M(T,H) = \frac{C_M(T,H)}{T} dT + \left(\frac{\partial M(T,H)}{\partial T}\right)_T dH$$

$$HeatFlow = -\Delta \breve{H}$$

$$d\breve{H} = \delta Q + V dP$$

$$\delta Q = T dS = C_P dT$$

$$\Delta C_P(T,H) = -\Delta C_M(T,H) = -T\left(\frac{\partial S_M}{\partial T}\right)$$

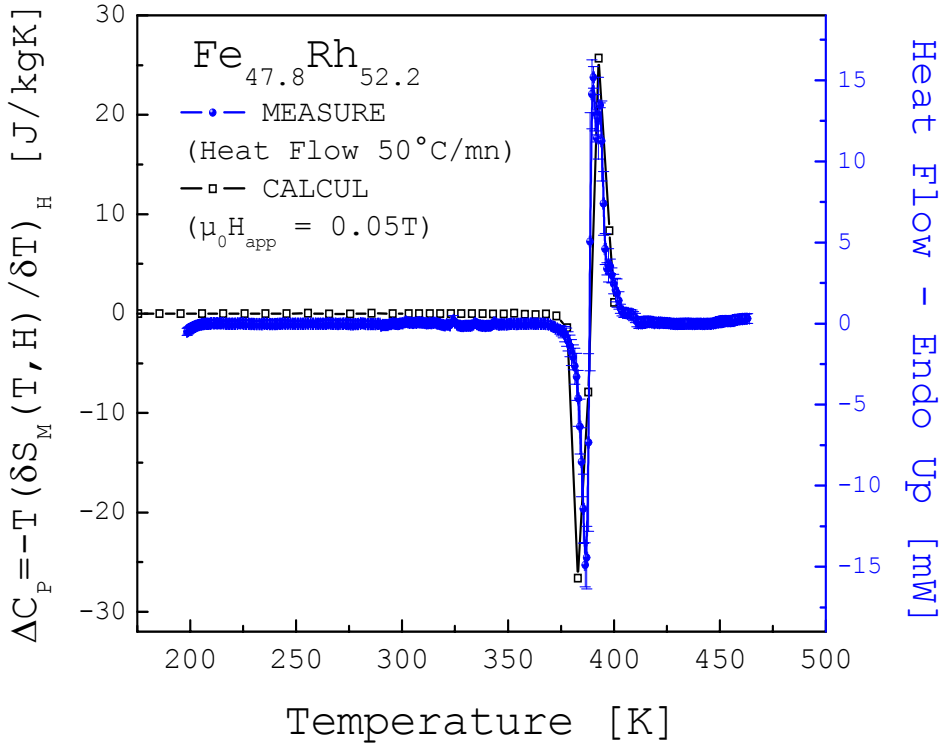

FeRh system

DSC vs Magnetic Measurements

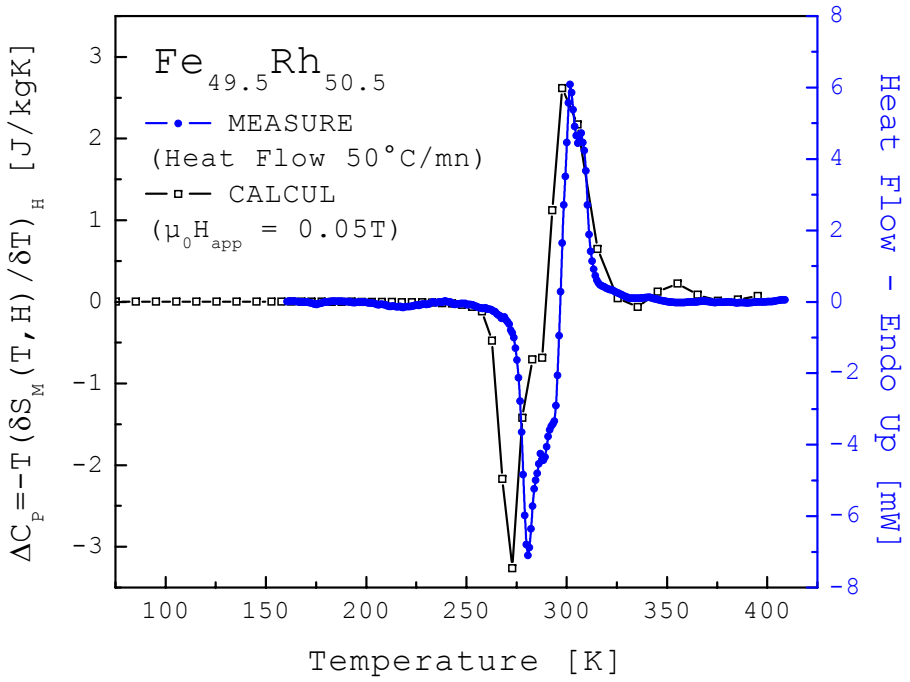

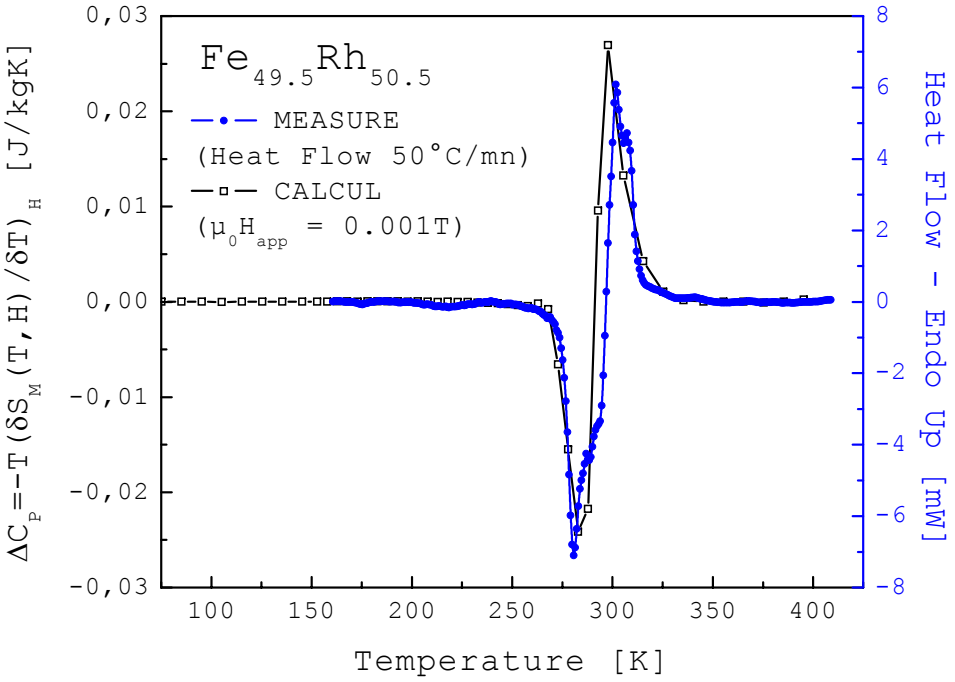

- Both thermomagnetic derived effect show good agreement
- The observed shift decreases sharply when the applied field is reduced

-
-
  -
  -
-
  -
  -
- The Hybrid FePt/FeRh system
-

The Hybrid FePt/FeRh system

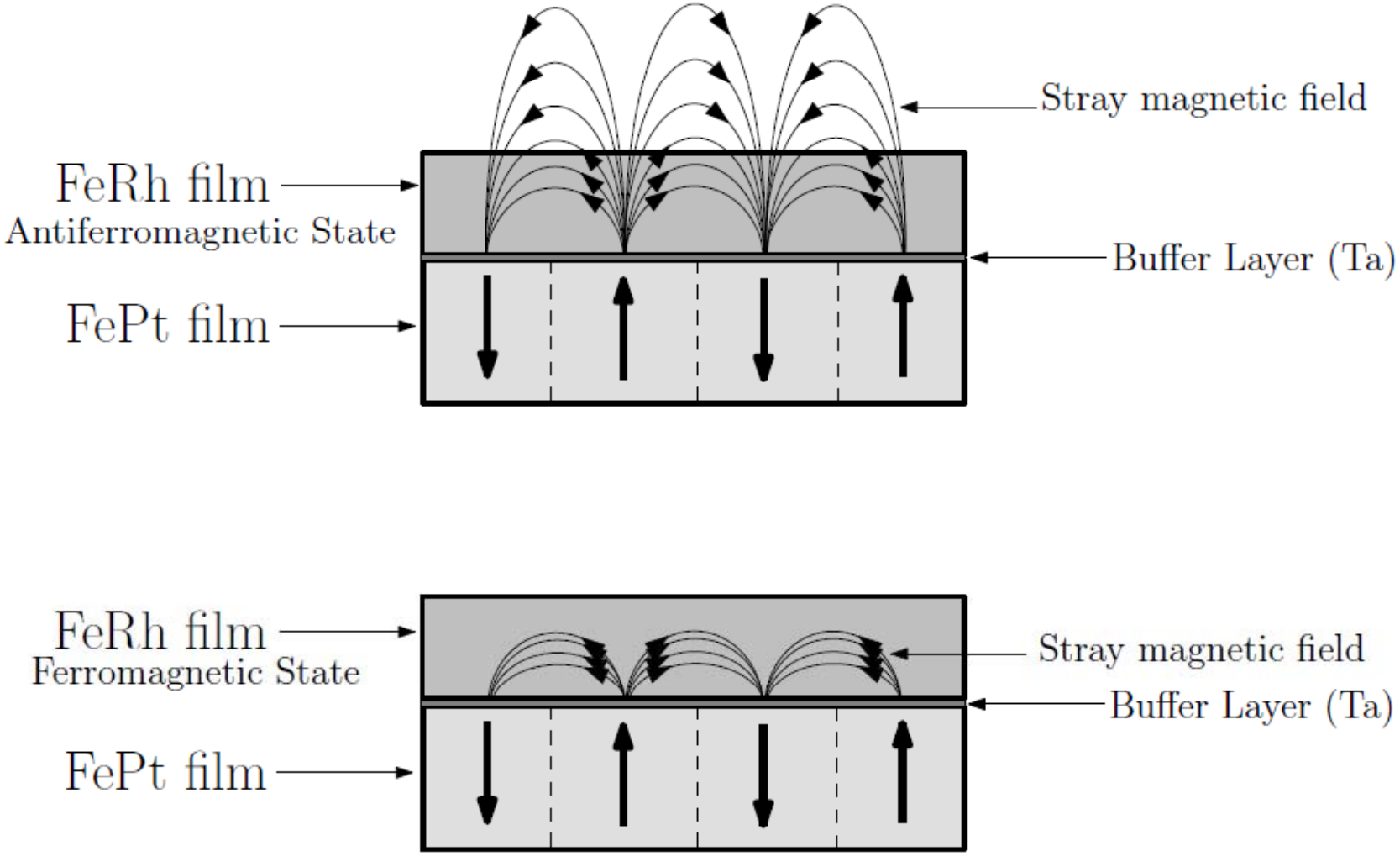

The Hybrid FePt/FeRh system

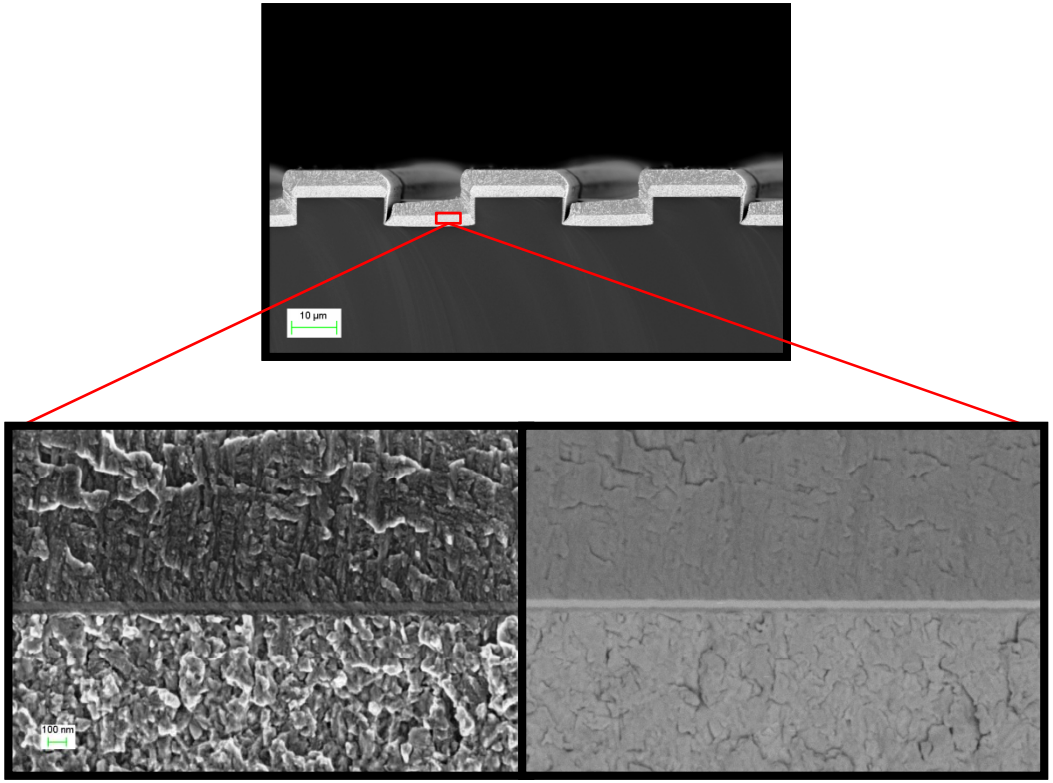

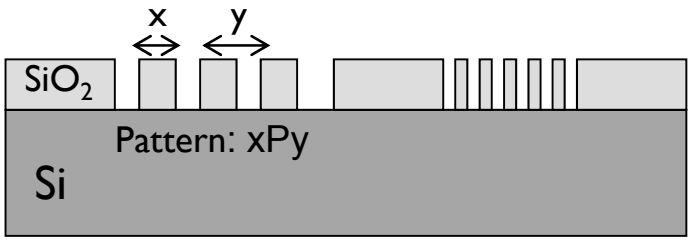

The substrate is pre-patterned with SiO_2 by lithography (the lateral dimensions are referenced by the width x and the periodicity y of the strips)

The Hybrid FePt/FeRh system

Magnetic characterization

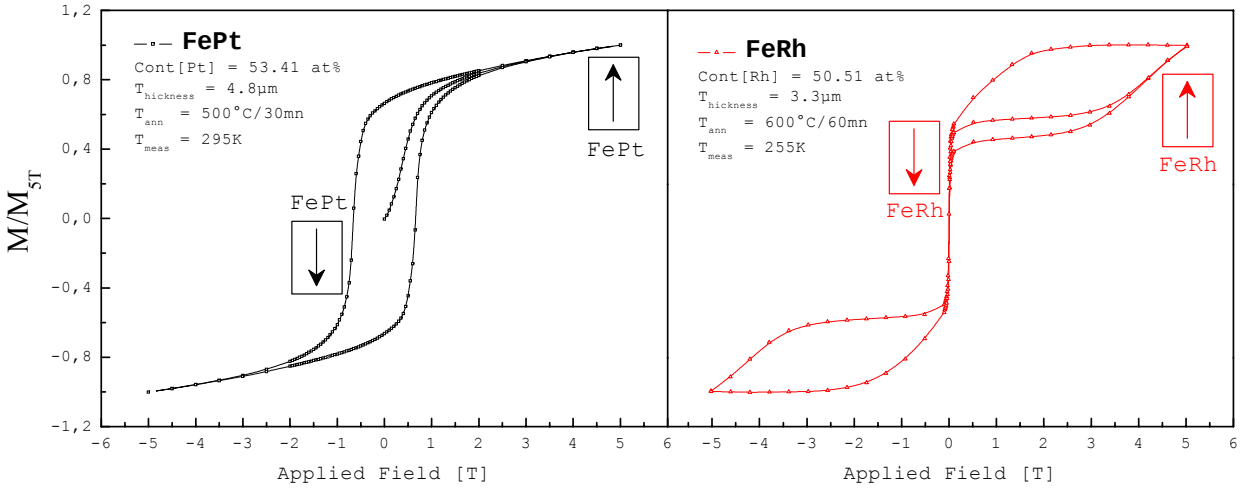

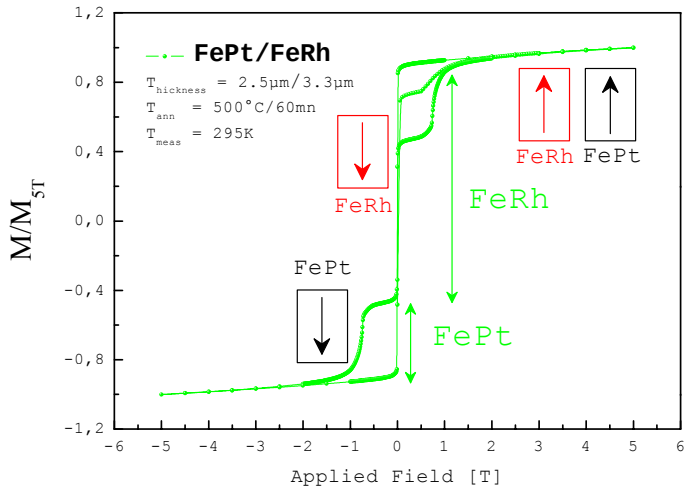

The magnetic signal obtained is a superposition of two magnetic contributions of sub-layers of FePt and FeRh.

The Hybrid FePt/FeRh system

Magneto-optic characterization

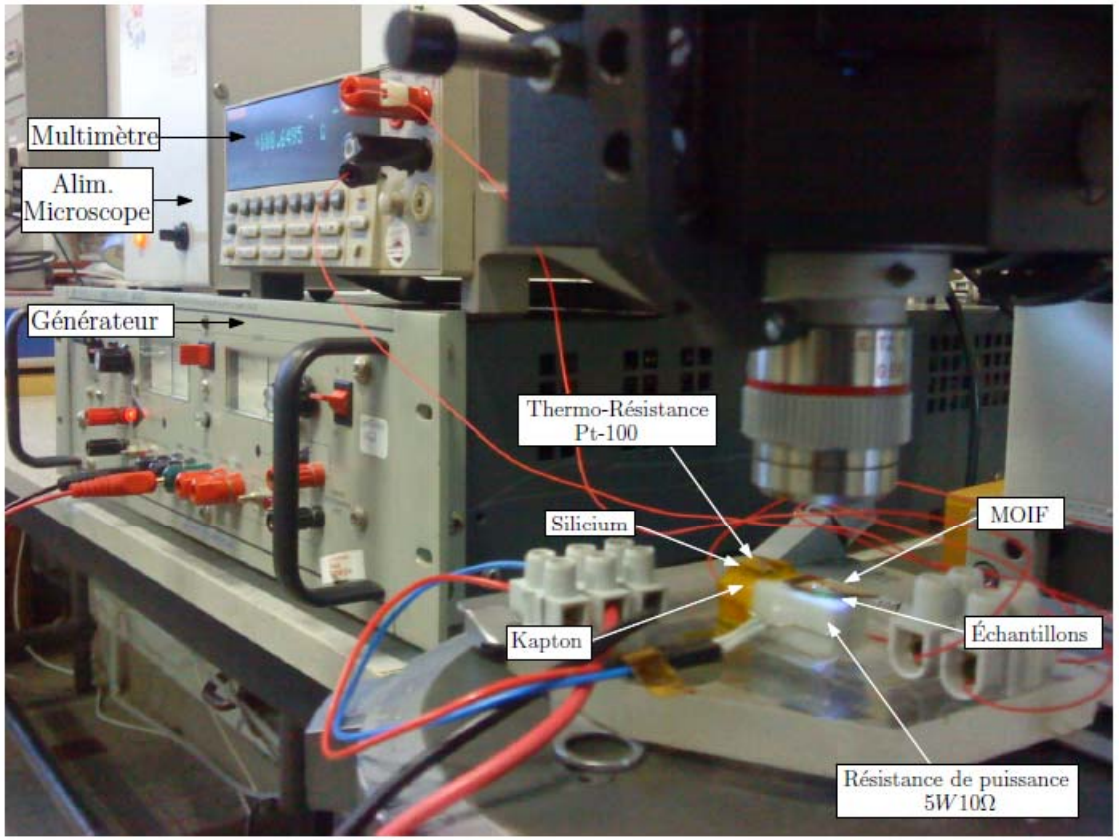

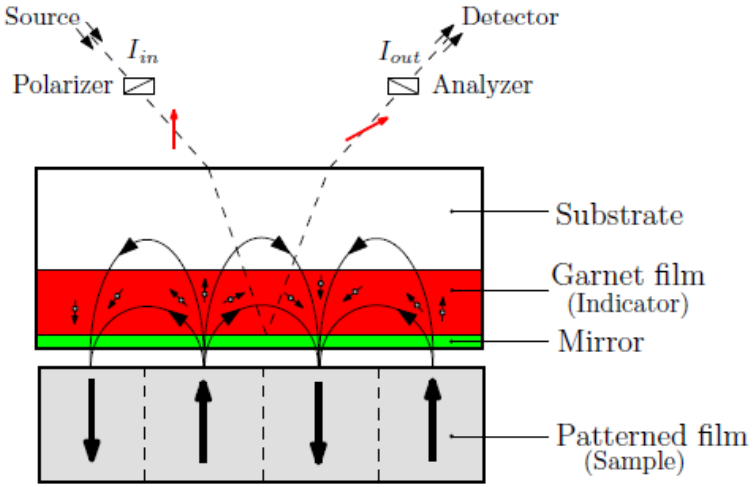

MOIF (Magneto Optical Indicator Film)

The Hybrid FePt/FeRh system

Magneto-optic characterization

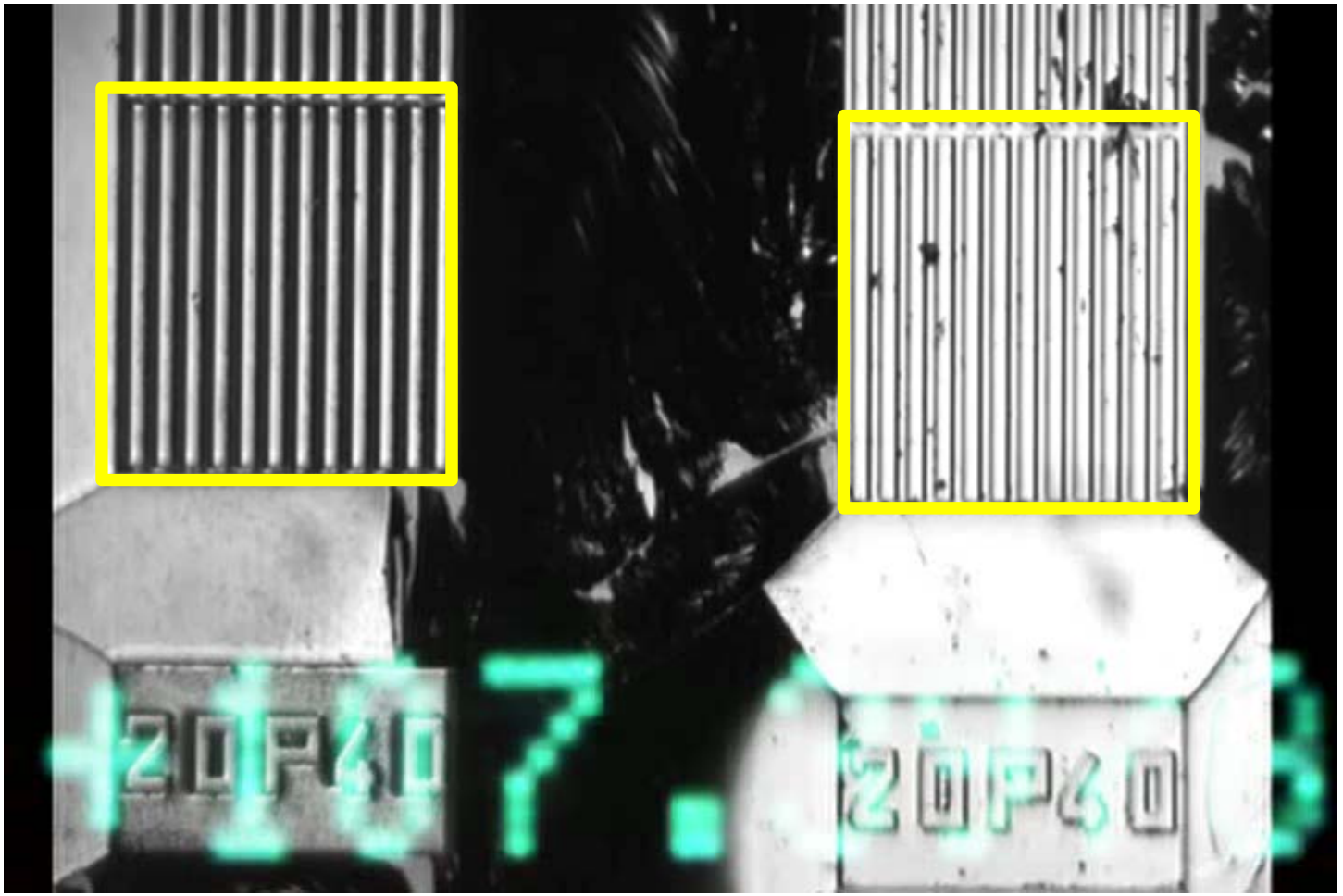

FePt/FeRh **FePt**

-
-
  -
  -
-
  -
  -
-
- Conclusions

Conclusions

Subtle links between structural and magnetic properties studied in FePt and FeRh

Quantitative analysis of magnetic and magneto-thermal properties carried out

Demonstration of a potential use of FeRh for magnetic screening

Perspectives

Broad range of possible applications of these functional magnetic materials in magnetic micro-systems

FePt particularly suited to bio-medical applications

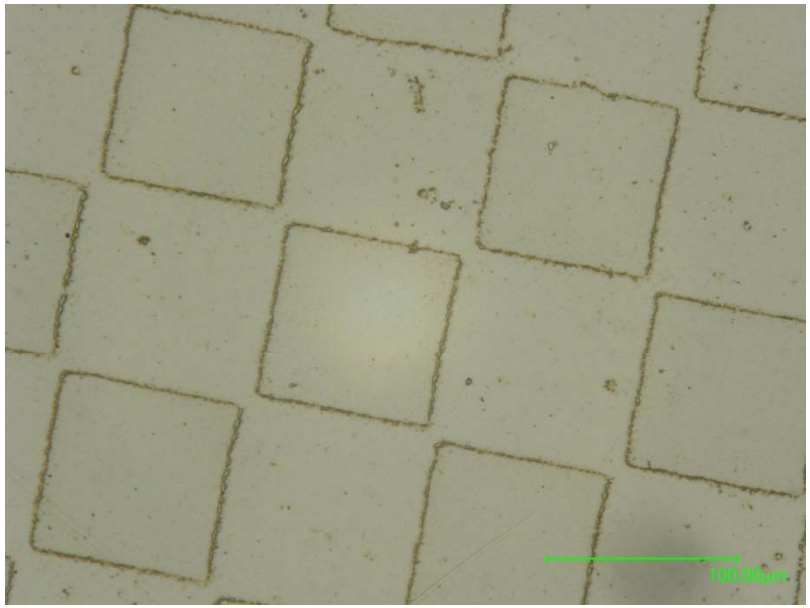

F. Dumas-Bouchiat + C. Ndao + A. Zaccaria (GIN)

Trapping of Fe-oxide nanoparticles on FePt film structured by Thermo-Magnetic-Patterning

Applications in selection / manipulation of biological species (cells, bacteria etc.)

Acknowledgments

Rostislav Grechishkin (Univ. TVER)
El-Kebir Hlil
Frédéric Dumas-Bouchiat
Laurent Ranno
Olivier Geoffroy

David Barral
Didier Dufeu
Laurent Del-Rey
Eric Eyraud
Denis Maillard

Philippe Plaindoux
Luc Ortéga

Franck Balestro
Vitoria Barthem
Richard Heattel
Gilbert Reyne